HHS Public Access

Author manuscript

Pflugers Arch. Author manuscript; available in PMC 2017 August 01.

Published in final edited form as:

Pflugers Arch. 2016 August ; 468(8): 1311–1332. doi:10.1007/s00424-016-1823-8.

Extracellular Cl^- regulates human SO_4^{2-}/anion exchanger SLC26A1 by altering pH-sensitivity of anion transport

Meng Wu[1,2,3], **John F. Heneghan**[3], **David H. Vandorpe**[3,4], **Laura I. Escobar**[5], **Bai-Lin Wu**[1,2], and **Seth L. Alper**[3,4]

[1]Ministry of Education Key Laboratory of Contemporary Anthropology, School of Life Sciences and Institutes of Biomedical Sciences, Fudan University, Shanghai 200433 China

[2]Division of Laboratory Medicine, Boston Children's Hospital, Boston, MA 02115

[3]Division of Nephrology and Department of Medicine, Beth Israel Deaconess Medical Center, Boston, MA 02215

[4]Department of Medicine, Harvard Medical School, Boston, MA 02115

[5]Department of Physiology, Faculty of Medicine, Universidad Nacional Autonoma de Mexico, Mexico DF 04510

Abstract

Genetic deficiency of the SLC26A1 anion exchanger in mice is known to be associated with hyposulfatemia and hyperoxaluria with nephrolithiasis, but many aspects of human SLC26A1 function remain to be explored. We report here the functional characterization of human SLC26A1, a DIDS-sensitive, electroneutral sodium-independent anion exchanger transporting sulfate, oxalate, bicarbonate, thiosulfate and (with divergent properties) chloride. Human SLC26A1-mediated anion exchange differs from that of its rodent orthologs in its stimulation by alkaline pH_o and inhibition by acidic pH_o but not pH_i, and in its failure to transport glyoxylate. SLC26A1-mediated transport of sulfate and oxalate is highly dependent on allosteric activation by extracellular chloride or nonsubstrate anions. Extracellular chloride stimulates apparent V_{max} of human SLC26A1-mediated sulfate uptake by conferring a two-log decrease in sensitivity to inhibition by extracellular protons, without changing transporter affinity for extracellular sulfate. In contrast to SLC26A1-mediated sulfate transport, SLC26A1-associated chloride transport is activated by acid pH_o, shows reduced sensitivity to DIDS, and exhibits cation-dependence of its DIDS-insensitive component. Human SLC26A1 resembles SLC26 paralogs in its inhibition by phorbol ester activation of PKC, which differs in its undiminished polypeptide abundance at or near the oocyte surface. Mutation of SLC26A1 residues corresponding to candidate anion binding site-associated residues in avian SLC26A5/prestin altered anion transport in patterns resembling those of prestin. However, rare SLC26A1 polymorphic variants from a patient with renal Fanconi Syndrome and from a patient with nephrolithiasis/calcinosis exhibited no loss-of-function phenotypes consistent with disease pathogenesis.

Contact: Seth L. Alper, MD-PhD, Nephrology Section and Vascular Biology Research Center, Beth Israel Deaconess Medical Center RN380F, 99 Brookline Ave, Boston, MA 02215, Tel: 617-667-2930, salper@bidmc.harvard.edu.

Keywords

oxalate transport; glyoxylate; protein kinase C; renal Fanconi Syndrome; nephrocalcinosis; *Xenopus* oocyte

Introduction

The highly conserved human *SLC26* gene family includes 11 members encoding at least 10 polypeptide gene products that mediate electroneutral or electrogenic anion transport in many cell and tissue types [15]. The SLC26 proteins are N-glycosylated [44] homodimers [14] (or tetramers [5,78]) with short N-terminal cytoplasmic domains followed by 14 transmembrane spans and C-terminal cytoplasmic STAS domains of variable length [3,24]. Mammalian SLC26 proteins transport small anion substrates including Cl^-, HCO_3^-, OH^-, SO_4^{2-}, oxalate, I^-, and formate [56], whereas SLC26-related SulP proteins transport dicarboxylates, as well [36,74], playing important roles in maintaining cellular anion homeostasis [15]. Human SLC26 mutations cause Mendelian diseases such as diastrophic (chondro)dysplasia (*SLC26A2*) [4], congenital chloride diarrhea (*SLC26A3*) [80], Pendred syndrome or isolated enlargement of the vestibular acqueduct (*SLC26A4*) [8,79], and impaired male fertility (*SLC26A8)* [21]. *SLC26A9* is a risk modifier gene for cystic fibrosis [9,77], and SLC26A11 polypeptide has been implicated in the neuronal swelling of cerebral edema [66]. In mice, genetically engineered loss of function led, in addition, to outer hair cell deafness (*Slc26a5*) [45]; oxalate urolithiasis *(Slc26a6, Slc26a1*) [18,34], and distal renal tubular acidosis (*Slc26a7, Slc26a9*) [83,84].

SLC26A1/SAT1 cDNA was first cloned from rat liver as a Na^+-independent SO_4^{2-} transporter [7]. Human SLC26A1 exhibits modest cross-species conservation of amino acid sequence, sharing 78% identity with rat SLC26A1 and 77% with mouse SLC26A1, but only 44% identity with paralogous human SO_4^{2-} transporter SLC26A2 [61]. Previous studies of human and rodent SLC26A1 have demonstrated electroneutral, pH-regulated exchange of anions including SO_4^{2-}, oxalate, HCO_3^-, thiosulfate, and glyoxylate, sensitive to inhibition by 4,4'-diisothiocyano-2,2'-stilbenedisulfonic acid (DIDS) [40-42,61,70,82]. However, the ability of SLC26A1 to transport Cl^- remains controversial, with reports both detecting [42,61] and failing to detect Cl^- transport [41,51,82]. An unusual property of rodent SLC26A1-mediated SO_4^{2-} uptake measured in Xenopus oocytes is cis-stimulation by extracellular Cl^-[69], as well as by other non-substrate anions, including Br^-, I^-, formate, and lactate [82]. The mechanism of this cis-stimulation has remained unclear.

SO_4^{2-} is an essential nutrient for development [16], biosynthetic sulfation [28]and hepatic sulfate conjugation reactions [25]. The widely expressed SLC26A1 is particularly abundant in sinusoidal membranes of hepatocytes and in basolateral membranes of intestinal enterocytes and renal proximal tubular cells, with higher expression in male than female rats [12,37,42,60-62]. The liver is also the main site of oxalate uptake from dietary absorption, oxalate biosynthesis from ascorbate and amino acid metabolism, and oxalate catabolism [53,76]. Hepatic SLC26A1 is the likely sinusoidal exchanger of intracellular oxalate for extracellular SO_4^{2-}, enabling SO_4^{2-} uptake and oxalate secretion for eventual excretion by

intestine and kidney [11]. Renal glomeruli freely filter both $SO_4$2− and oxalate. Most filtered SO_4^{2-} is reabsorbed by renal proximal tubular cells, which also secrete oxalate [6,32,38,71]. SLC26A1 in proximal tubular cell basolateral membrane likely mediates basolateral SO_4^{2-} efflux into the pericapillary interstitial space, in exchange for uptake of extracellular oxalate, which can then be secreted across the apical membrane by SLC26A6 [48].

Slc26a1$^{-/-}$ mice exhibited urolithiasis, hyperoxaluria, hyperoxalemia, hyposulfatemia, hypersulfaturia, and increased susceptibility to hepatotoxicity [18]. However, oxalate secretion by isolated *Slc26a1*$^{-/-}$ duodenum was unchanged [39], and Slc26a1 mRNA and protein abundance was unaltered in mice with hyperoxaluria of other causes, questioning the physiological role of SLC26A1 in hyperoxaluria (at least in duodenum) [23]. Human diseases caused by SLC26A1 mutations have not been reported.

In the present study, we further delineate the function and regulation of human SLC26A1 expressed in *Xenopus* oocytes, and test potential pathogenicity of selected candidate disease-associated missense variants. We report that extracellular Cl^- allosterically activates SLC26A1 by increasing SLC26A1 V_{max} for SO_4^{2-} transport without change in $K_{1/2}$ for $SO_4^{2-}{}_{[o]}$. The increased V_{max} reflects a 2 log decrease in sensitivity of SO_4^{2-}/anion exchange to inhibition by extracellular protons.

Methods

Materials

Na36Cl and H36Cl were from ICN (Irvine, CA) and $Na_2{}^{35}SO_4$ from ARC (Saint Louis, MO). ^{14}C-oxalate originally from NEN-DuPont (Boston, MA) was a gift from C. Scheid and T. Honeyman (Univ. Mass. Med. Ctr.). Restriction enzymes and T4 DNA ligase were from New England Biolabs (Beverly, MA). EXPAND High-fidelity PCR System was from Roche Diagnostics (Indianapolis, IN). QuikChange II XL site-directed mutagenesis kit was from Agilent Technologies (Lexington, MA). MEGAscript® T7 Transcription Kit was from Thermo Fisher Scientific (Waltham, MA). 4,4'-Diisothiocyanostilbene-2,2'-disulfonic acid (DIDS) was from Calbiochem (La Jolla, CA). Phorbol-12-myristate-13-acetate (PMA) was from LC Laboratories (Woburn, MA). Niflumic acid (NFA), glyoxylate, dibutyryl cyclic AMP sodium salt (dB-cAMP), 3-Isobutyl-1-methylanxthine (IBMX), tenidap and 1,2-Bis(2-aminophenoxy)ethane -N,N,N’,N’-tetraacetic acid tetrakis (acetoxymethyl ester) (BAPTA-AM) were from Santa Cruz Biotechnology (Dallas, TX). Hydrochlorothiazide (HCTZ) and R-(+)-[(2-n-Butyl-6,7-dichloro-2-cyclopentyl-2,3-dihydro-1-oxo-1H-inden-5-yl)oxy]-acetic acid (DIOA) were from Sigma (St. Louis, MO). DMSO Stock solutions of these drugs were stored at −20 °C. All other chemical reagents were from Sigma or Fluka (Milwaukee, WI) and were of reagent grade.

Solutions

Modified Barth's saline (MBS) consisted of (in mM) 85 NaCl, 1 KCl, 2.4 $NaHCO_3$, 0.82 $MgSO_4$, 0.33 $Ca(NO3)_2$, 0.41 $CaCl_2$, and 10 HEPES (pH adjusted to 7.40 with NaOH). ND96(Cl^-) (referred to in cation substitution experiments as ND96(Na+)) consisted of (in

mM) 96 NaCl, 2 KCl, 1.8 $CaCl_2$, 1 $MgCl_2$, and 5 HEPES, adjusted to 7.40. In Cl^--free ND96 or partial Cl^- substitution solutions, NaCl was replaced mole-for-mole with other sodium salts (substituted anion in parentheses: e.g. ND96(gluconate)) or with mannitol. In all Cl^--free ND96 solutions, KCl, $CaCl_2$, and $MgCl_2$ were substituted with the corresponding gluconate salts. In Na^+-free ND96, NaCl was replaced by mole-for-mole with KCl or N-methyl-D-glucamine (NMDG-Cl; described with the substituted cation in parentheses: e.g. ND96(K^+)). Oxalate-containing bath solutions were nominally free of Ca^{2+} and Mg^{2+}. Addition of sodium butyrate (40 mM) was in mole-for-mole substitution for NaCl. ND96 solutions at pH 5.0 and pH 6.0 were buffered with 5 mM MES. ND96 solutions at pH values of 8.0 through 9.5 were buffered with 5 mM tricine.

Construction and mutagenesis of cDNA expression plasmids

Human SLC26A1 (NM_022042) was subcloned into the Xenopus oocyte expression vector pXT7. pXT7-SLC26A1 with a fused N-terminal HA-tag was constructed by PCR mutagenesis and ligation. SLC26A1 mutations C41W, A56T, M132T, E295Q, A400C, K401E, and Q556R were generated by QuikChange II XL site-directed mutagenesis kit using specific mutagenic oligonucleotides. (See Table S1 for oligonucleotide primer sequences).

Expression of cRNA in Xenopus oocytes

SLC26A1 cRNA and Xenopus oocytes were prepared as previously described [31]. Oocytes injected with 50 nl cRNA (1-40 ng) and uninjected oocytes were maintained at 17.5°C in MBS containing gentamicin for 2-5 days before use. Control uninjected and control water-injected oocytes exhibited indistinguishable levels of influx of $36Cl^-$, of $^{35}SO_4^{3-}$, and of 14C-oxalate (data not shown).

Isotopic influx experiments

Oocytes were prewashed (<1 min) in radioisotope-free influx medium to avoid introduction of trace (Cl^--containing) MBS to the influx assay. $^{35}SO_4^{2-}$ influx assays were of 30 min duration (or as indicated) in ND96(Cl^-) or in Cl^--free ND96 bath solutions containing 1 mM (2 μCi) $^{35}SO_4^{2-}$ (or as indicated) in 150 μl volumes in microtiter plate wells. $^{36}Cl^-$ influx studies of 30 min duration were carried out in ND96(Na^+), ND96 (K^+) or ND96(NMDG), or in other bath solutions as indicated. Total bath [Cl^-] was 103.6 mM (0.25 μCi/well). $K^{36}Cl$ was used in Na^+-free baths. ^{14}C-oxalate influx studies were carried out for 30 min periods in nominally Ca^{2+}- and Mg^{2+}-free ND96(Cl^-) with 1.0 mM sodium ^{14}C-oxalate (0.375 μCi/well; 150 μl). Chemicals and drugs were diluted to the indicated concentrations in influx bath solution before uptake experiments. Influx experiments were terminated with 3 washes in cold ND96(cyclamate), followed by oocyte lysis in 150 μl of 2% sodium dodecyl sulfate (SDS). Duplicate 10μl aliquots of influx solution (in 150 μl 2% SDS) were used to calculate specific activities of radiolabeled substrate anions. Oocyte anion uptake was calculated from oocyte-associated counts per minute (cpm) and bath specific activity.

Isotopic efflux experiments

For $^{35}SO_4^{2-}$ efflux studies, individual oocytes were injected with 50 nl $Na_2{}^{35}SO_4$ (5,000~8,000 cpm). After a 5- to 10-min recovery period in ND96 (gluconate), the $^{35}SO_4^{2-}$ efflux assay was initiated by transfer of individual oocytes to 6 ml borosilicate glass tubes, each containing 1 ml efflux solution. At intervals of 1 or 3 min, 0.95 ml of this efflux solution was removed for scintillation counting and replaced with an equal volume of fresh efflux solution. After completion of the assay with a final efflux period in the presence of the inhibitor 200 μM DIDS, each oocyte was lysed in 150 μl of 2% SDS for counts of residual oocyte-associated radioisotope.

For $^{36}Cl^-$ efflux studies, oocytes were injected with 50 nl of 40 mM $Na^{36}Cl$ (5,000 −8,000 cpm). After 5 min recovery in ND96(gluconate), oocytes were transferred into fresh efflux solutions and the assay was carried out as above. For ^{14}C-oxalate efflux assays, oocytes were injected with 50 nl of 100 mM $Na^{14}C$-oxalate (8,000-10,000 cpm, with final estimated intracellular concentration 10 mM). After a recovery period of at least 15 min, efflux was measured as above.

To vary oocyte pH_i, oocytes were pre-exposed to 40 mM Na butyrate (substituting for NaCl) for 30 min before initiation of an efflux experiment to produce intracellular acidification of 0.5 pH units to pH_i ~6.7-6.8 [75]. Upon removal of bath butyrate (with substitution by NaCl) during the efflux experiment, pH_i alkalinized back toward initial pH_i while pH_o remained constant.

Efflux data were plotted and anion efflux rate constants were calculated as previously reported [31].

Confocal immunofluorescence microscopy

Three or four days after injection with cRNA encoding wild-type or mutant HA-SLC26A1, 10–12 oocytes were fixed with 1.5% paraformaldehyde (PFA) in phosphate-buffered saline (PBS) for 30 min at room temperature and washed three times with PBS containing 0.002% Na azide (PBS-azide). Oocytes were then placed in PBS containing 1% SDS for 15 min to further permeabilize the surface membrane and unmask epitopes. After three subsequent washes in PBS-azide, oocytes were blocked for 1h in PBS containing 1% bovine serum albumin (PBS-BSA), then washed three times with PBS-BSA.

Fixed, permeabilized, and blocked oocytes were incubated overnight at 4°C with rabbit monoclonal anti-HA antibody (Cell Signaling Technologies, Danvers, MA) diluted 1:1000 in PBS-BSA, then washed three times in cold PBS-BSA. Antibody-labeled oocytes were then incubated 2-3 h at room temperature with Cy3-conjugated secondary goat anti-rabbit Ig (diluted 1:500, Jackson ImmunoResearch, West Grove, PA), again thoroughly washed in PBS-BSA, and stored at 4°C until imaging. Cy3-labeled oocytes were imaged using previously reported confocal microscope settings and parameters [31]. Polypeptide abundance at or near the oocyte surface was estimated by Image J quantitation of fluorescence intensity as previously described [31].

Statistics

Data were reported as means ± SE. Flux data were compared by Student's paired or unpaired two-tailed t tests, or by ANOVA with Tukey post-hoc analysis (SPSS). Some concentration-dependence datasets were fit to the Michaelis-Menten equation using GraphPad Prism.

Results

SLC26A1 mediates $SO_4^{2-}{}_{[i]}/SO_4^{2-}{}_{[o]}$ exchange

SLC26A1-mediated $^{35}SO_4^{2-}$ uptake remained linear for >30 min (Fig. 1a inset) and was maximal in oocytes previously injected with ≥ 5 ng SLC26A1 cRNA (Fig. 1a). In these conditions, SLC26A1-mediated $^{35}SO_4^{2-}$ influx exhibited a $K_{1/2}$ for $SO_4^{2-}{}_{[o]}$ of 0.26±0.04 mM, with maximal influx at ≥ 1 mM extracellular SO_4^{2-} ($SO_4^{2-}{}_{[o]}$) (Fig. 1b). Accordingly, in most of the following $^{35}SO_4^{2-}$ influx experiments oocytes were injected with 5 ng cRNA, influx bath solutions contained 1 mM SO_4^{2-}, and influx time period was 30 min. Efflux of $^{35}SO_4^{2-}$ from SLC26A1 expressing oocytes increased ~4-fold upon addition of 1 mM SO_4^{2-} to a Cl^- bath, and this increment was abrogated by addition of 200 μM DIDS (Fig. 1c,d), consistent with SLC26A1-mediated $^{35}SO_4^{2-}{}_{[i]}/SO_4^{2-}{}_{[o]}$ exchange. Two electrode voltage clamp experiments performed in Cl^- bath and in cyclamate bath (Fig. S1) detected no evidence for SLC26A1-mediated electrogenic influx of SO_4^{2-}, consistent with previous reports [40].

Alkaline pH_o stimulates SLC26A1-mediated SO_4^{2-} flux

SLC26A1 was sensitive to pH_o. $^{35}SO_4^{2-}$ uptake by SLC26A1-expressing oocytes at pH_o 5.0 was lower than at pH_o 7.4, whereas $^{35}SO_4^{2-}$ uptake at pH_o 8.5 was higher than at pH_o 7.4 (Fig. 2a). Alkaline pH_o-stimulated, DIDS-sensitive $^{35}SO_4^{2-}$ efflux from SLC26A1-expressing oocytes was evident also in $SO_4^{2-}{}_{[o]}$-free ND96(Cl^-) and in ND96(gluconate) bath solutions at pH_o 8.5 (Fig. 2b-e). The $Cl^-{}_{[o]}$-independence of $^{35}SO_4^{2-}$ efflux was consistent with exchange of intracellular SO_4^{2-} for extracellular OH^-. The pH_o dependence of SLC26A1-associated $SO_4^{2-}{}_{[i]}/SO_4^{2-}{}_{[o]}$ exchange (measured in Cl^- bath) was consistent with a single major protonation site regulating transport (Fig. 2f,g). pH_i did not regulate SLC26A1-mediated $^{35}SO_4^{2-}{}_{[i]}/SO_4^{2-}{}_{[o]}$ exchange in Cl^- bath, as judged by the lack of change in efflux during reversible intracellular acidification of ~0.5 units [75] elicited by exposure to and removal of sodium butyrate (Fig. 2h,i). These data together suggested that SLC26A1 can mediate alkaline pH_o-stimulated and acid pH_o−inhibited $^{35}SO_4^{2-}/SO_4^{2-}$ exchange and likely also $^{35}SO_4^{2-}[i]/^{OH-}[o]$ exchange.

$Cl^-{}_{[o]}$ cis-stimulates SLC26A1-mediated SO_4^{2-} transport

Previous data have suggested cis-stimulation of SLC26A1-mediated $^{35}SO_4^{2-}$ uptake by halides and other anions [42,69,82], and more extensive evidence for Cl^- regulation of SLC26A2 activity has been presented [55,69]. We found that human SLC26A1-mediated $^{35}SO_4^{2-}$ uptake in Xenopus oocytes was nearly completely dependent upon extracellular anions, as previously noted for mouse [42] and eel SLC26A1 [51]. The $[Cl^-]_o$-dependence of $^{35}SO_4^{2-}$ uptake (measured in the presence of isosmotic mannitol substitution)

exhibited a $K_{1/2}$ for $Cl^-_{[o]}$ of 13.3 mM (R^2=0.81; Fig. 3a). Measured in the presence of isosmotic gluconate substitution, $^{35}SO_4^{2-}$ uptake did not absolutely require Cl^-, and the $[Cl^-]_o$-dependence of the gluconate-stimulated incremental fraction of $^{35}SO_4^{2-}$ uptake displayed a $K_{1/2}$ of 8.33 mM (R^2=0.4; Fig. 3b).

As shown in Fig. 3c,d, the slow $^{35}SO_4^{2-}$ efflux from SLC26A1-expressing oocytes into ND96(gluconate) containing 1 mM SO_4^{2-} was greatly accelerated by bath change from gluconate to Cl^-. In contrast, $^{35}SO_4^{2-}$ efflux from SLC26A1-expressing oocytes into baths of SO_4^{2-}-free ND96(gluconate) or SO_4^{2-}-free ND96(Cl^-) (both pH 7.4) was minimal and DIDS-insensitive (Fig. 3e,f). These results demonstrate that SLC26A1 fails to mediate $^{35}SO_4^{2-}{}_{[i]}/Cl^-_{[o]}$ exchange, and that the stimulatory effect of $Cl^-_{[o]}$ on $^{35}SO_4^{2-}{}_{[i]}/SO_4^{2-}{}_{[o]}$ exchange likely represents allosteric regulation of SLC26A1.

The mechanism by which $Cl^-_{[o]}$ exerts cis-stimulation on SLC26A1-mediated $^{35}SO_4^{2-}$ influx was subjected to more detailed investigation. Since multiple anions can cis-stimulate SLC26A1-mediated SO_4^{2-} transport ([82]; see also Fig. 3b and Fig. 4b) we tested the hypothesis that $Cl^-_{[o]}$ might modify SLC26A1 affinity for $SO_4^{2-}{}_{[o]}$. However, the SLC26A1 $K_{1/2}$ value for [SO_4^{2-}] was 0.24 ± 0.029 mM (R^2=0.78) as measured in ND96(Cl^-) and 0.24 ± 0.035 mM (R^2=0.68) as measured in ND96(gluconate) (Fig. 3g), demonstrating that $Cl^-_{[o]}$ does not regulate the apparent affinity of SLC26A1 for $SO_4^{2-}{}_{[o]}$. However, as shown in Fig. 3h, extracellular anions regulated the sensitivity of SLC26A1-mediated $^{35}SO_4^{2-}$ uptake to extracellular pH. The apparent proton affinity of SLC26A1 (as measured by $^{35}SO_4^{2-}$ uptake) was left-shifted by approximately two orders of magnitude by ND96(Cl^-) as compared to uptake in ND96(gluconate) (Fig. 3h). These experiments show that extracellular anions mediate allosteric regulation of the pH_o-sensitivity of SLC26A1-mediated $^{35}SO_4^{2-}$ influx (likely exchange), and that regulation likely explains the cis-stimulatory effect of $Cl^-_{[o]}$ on uptake of $^{35}SO_4^{2-}$ by SLC26A1.

Cyclamate inhibition of SLC26A1-mediated SO_4^{2-} influx is Cl^--dependent

SO_4^{2-} uptake from ND96(Cl^-) was compared to that from a range of Cl^--free bath solutions. As shown in Fig. 4a, $^{35}SO_4^{2-}$ uptake was slightly reduced in ND96(gluconate) and ND96(isethionate), and substantially reduced in ND96(cyclamate). In contrast (not shown), $^{35}SO_4^{2-}$ uptake in Cl^--free bath solutions of sulfamate, methanesulfonate, nitrate and phosphate was comparable in rate to that in ND96(Cl^-). Moreover, multiple sulfonate ("Good") buffers [26], at 40 mM concentrations failed to reduce SLC26A1-mediated $^{35}SO_4^{2-}$ uptake (Fig. S2).

The inhibitory effect of cyclamate on SO_4^{2-} transport might reflect direct inhibition at the putative SO_4^{2-} transport site, or reduced cis-stimulation at the hypothetical "cis-stimulatory anion site". Therefore, $^{35}SO_4^{2-}$ uptake was measured in a 1 mM SO_4^{2-} bath containing constant 56 mM Cl^- (producing maximal cis-stimulation; see Fig. 3a) plus osmotically balancing concentrations of D-mannitol, gluconate, or cyclamate. $^{35}SO_4^{2-}$ uptake was minimally impacted by bath substitution of 48 mM Cl^- with 96 mM D-mannitol or 48 mM gluconate, whereas substitution with 48 mM cyclamate decreased $^{35}SO_4^{2-}$ uptake significantly (Fig. 4b). However, bath change from ND96(gluconate) to ND96(cyclamate) did not inhibit SLC26A1-mediated, DIDS-sensitive $^{35}SO_4^{2-}{}_{[i]}/SO_4^{2-}{}_{[o]}$ exchange in Cl--free

bath (Fig. 4c,d). In contrast, $^{35}SO_4^{2-}{}_{[i]}/SO_4^{2-}{}_{[o]}$ exchange in ND96(Cl^-) bath was strongly and reversibly inhibited by bath cyclamate substitution (Fig. 4e,f), suggesting preferential inhibition by cyclamate of Cl^- action at the cis-stimulatory anion site, in addition to weaker binding or reduced agonism of cyclamate compared to Cl^- at the putative regulatory site.

SLC26A1 mediates oxalate transport

Oocyte expression of SLC26A1 increased ^{14}C-oxalate uptake by almost 20-fold compared with that by uninjected oocytes (Fig. 5a). To prevent bath oxalate chelation, the oxalate influx assay was performed in the nominal absence of both Ca^{2+} and Mg^{2+}, a condition which did not detectably affect influx of $^{35}SO_4^{2-}$ from either ND96(Cl^-) or ND96(gluconate) baths (Fig. S3). Bath addition of 5mM oxalate to ND96(Cl^-) increased DIDS-sensitive $^{35}SO_4^{2-}$ efflux from SLC26A1-expressing oocytes 3-fold (Fig. 5b,c), demonstrating $^{35}SO_4^{2-}{}_{[i]}/oxalate_{[o]}$ exchange mediated by SLC26A1. In contrast, however, oocytes previously injected with ^{14}C-oxalate exhibited no detectable DIDS-sensitive $oxalate_{[i]}/SO_4^{2-}{}_{[o]}$ exchange or $oxalate_{[i]}/Cl^-{}_{[o]}$ exchange, and the component of ^{14}C-oxalate efflux detected also appeared DIDS-insensitive (Fig. 5d,e).

Oocyte-expressed SLC26A1 mediates $SO_4^{2-}{}_{[i]}/HCO3^-{}_{[o]}$ exchange and $SO_4^{2-}{}_{[i]}/thiosulfate_{[o]}$ exchange, but not detectable $SO_4^{2-}{}_{[i]}/glyoxylate_{[o]}$ exchange

DIDS-sensitive $^{35}SO_4^{2-}$ efflux from SLC26A1-expressing oocytes was stimulated by bath addition of either 24mM HCO_3^- (Fig. 6a,b) or 5mM thiosulfate (Fig. 6c,d), demonstrating SLC26A1-mediated $^{35}SO_4^{2-}{}_{[i]}/HCO_3^-{}_{[o]}$ exchange and $^{35}SO_4^{2-}{}_{[i]}/thiosulfate_{[o]}$ exchange. Glyoxylate was previously identified as a substrate of rat SLC26A1 expressed in Xenopus oocytes [70]. However, 10mM bath glyoxylate failed either to stimulate efflux of $^{35}SO_4^{2-}$ from SLC26A1-expressing oocytes (Fig. 6e,f) or to cis-inhibit SLC26A1-mediated $^{53}SO_4^{2-}$ uptake (Fig. 6g). These data suggest that under the conditions tested in the current study, glyoxylate is not a substrate of human SLC26A1.

Acid pH_o stimulates Cl^- flux in SLC26A1 expressing oocytes

Cl^- has been reported to be a substrate of both mouse and human SLC26A1 polypeptides. We therefore compared pH sensitivity of SLC26A1-associated $36Cl^-$ flux with that of SLC26A1-mediated $^{35}SO_4^{2-}$ flux. Since oocytes previously injected with 5 ng SLC26A1 cRNA exhibited low Cl^- transport rates, these Cl^- transport experiments were performed with oocytes previously injected with 40 ng cRNA, and exhibited substantial Cl^- influx. However, in contrast to the pH-dependence of SLC26A1-mediated $^{35}SO_4^{2-}$ influx, $36Cl^-$ influx associated with SLC26A1 was significantly higher at pH_o 5.0 than at more alkaline pH_o values (Fig. 7a). SLC26A1-associated efflux of $^{36}Cl^-{}_{[i]}$ was similarly activated by acidic pH_o and comparatively inhibited by more alkaline bath pH_o values, whether in the presence of ND96(Cl^-) or ND96(gluconate) (Fig. 7b-e), and independent of the order of exposure to acid and alkaline pH_o conditions (Fig. S4). Although the pH_o-dependence of $^{36}Cl^-$ influx is compatible with $Cl^-{}_{[o]}/OH^-{}_{[i]}$ exchange, the similar pH_o-dependence of Cl^- efflux is not compatible with this transport mechanism. Thus, the stimulatory effects of protons on SLC26A1-associated $^{36}Cl^-$ transport may reflect an allosteric regulation by pH that differs from pH_o-dependent regulation of SO_4^{2-} transport.

$Cl^-_{[o]}$ stimulates $Cl^-_{[i]}$ efflux in SLC26A1-expressing oocytes

Our detection of $^{36}Cl^-$ efflux by SLC26A1-expressing oocytes (Fig. 7) prompted further investigation of this Cl^- transport process. $^{36}Cl^-$ efflux from these SLC26A1-expressing oocytes (40 ng cRNA) into SO_4^{2-}-free ND96(gluconate) was accelerated upon bath change to ND96(Cl^-) (Fig. 8a,b), consistent with $Cl^-_{[i]}/Cl^-_{[o]}$ exchange (or with regulatory stimulation by Cl^-_o of non-exchange Cl^- efflux). However, bath change from SO_4^{2-}-free ND96(Cl^-) to nominally Cl^--free 64 mM SO_4^{2-} retarded but did not abolish efflux of $36Cl^-$ (Fig. 8c,d), consistent with $36Cl^-_{[i]}/SO_4^{2-}{}_{[o]}$ exchange at low rates and with reduced DIDS-sensitivity (Figs 7, 8).

SLC26A1-mediated transport of SO_4^{2-} and Cl^- differ in $Na+_{[o]}$ dependence

Although SLC26A1 mediated substantial rates of Cl^- influx (Fig. 7a), neither $SO_4^{2-}{}_{[i]}/Cl^-_{[o]}$ exchange nor $Cl^-_{[i]}/SO_4^{2-}{}_{[o]}$ exchange mediated by SLC26A1 were detected (Fig. 3 and 8). SLC26A1-mediated $^{35}SO_4^{2-}$ uptake was Na^+-independent (Fig. 9a), as previously reported [7,69,82]. In contrast, SLC26A1-associated Cl^- influx exhibited a complex cation dependence (Fig. 9b). $^{36}Cl^-$ uptake by SLC26A1-expressing oocytes was lower in ND96(NMDG) than in either ND96(Na^+) or in ND96(K^+). Moreover, whereas the Na^+-dependent component of $^{36}Cl^-$ uptake (~45%) was DIDS-sensitive, the remaining, DIDS-insensitive component of uptake was comparable in magnitude to $^{36}Cl^-$ uptake in the absence of Na^+ (Fig. 9b). This contrasts to the abolition of SLC26A1-mediated SO_4^{2-} uptake by 200 μM DIDS (Fig. 9a), even in oocytes previously injected with 40 ng cRNA (data not shown). SLC26A1-associated $^{36}Cl^-$ influx from ND96(Na^+) was completely insensitive to 100 μl HCTZ and to 500 μM DIOA, suggesting that neither activation of endogenous oocyte Na^+-Cl^- cotransport nor of oocyte K^+-Cl^-cotransport accounted for the observed SLC26A1-associated Na^+-dependent Cl^- flux. SLC26A1-associated $^{36}Cl^-$ flux was also insensitive to 200 μM niflumic acid (NFA, Fig. 9c), in contrast to its partial sensitivity to 200 μM DIDS, and arguing against endogenous NFA-sensitive anion channels as mediators of SLC26A1-associated Cl^- transport.

SLC26A1 is inhibited by PKC

Several SLC26A1 family members are sensitive to PKC [31,63], and SLC26A1 has several potential PKC phosphorylation sites. As shown in Fig. 10a,b, $^{35}SO_4^{2-}{}_{[i]}/SO_4^{2-}{}_{[o]}$ exchange mediated by either SLC26A1 or HA-tagged SLC26A1 was strongly inhibited after oocyte exposure to the classical PKC activator, PMA, whereas DMSO exposure had no effects (data not shown). PKC inhibition of SLC26A1 did not reflect decreased expression at or near the oocyte surface (Fig. 10c), in contrast to PMA-mediated reduction in oocyte surface expression accompanying PMA-medicated inhibition of SLC26A2 [31].

Manipulations of cAMP and intracellular Ca^{2+} did not alter SLC26A1 activity

SLC26A1-mediated $^{35}SO_4^{2-}$ uptake from ND96(Cl^-) or from ND96(gluconate) was not altered by oocyte treatment with dibutyryl-cAMP(dB-cAMP) and/or isobutylmethylxanthin (IBMX, Fig. S5a). Intracellular Ca^{2+} chelation by prolonged preincubation in BAPTA-AM or by preinjection with Na-EGTA similarly failed to alter SL26A1-mediated $^{35}SO_4^{2-}$ uptake from either ND96(Cl^-) or ND96(gluconate) (Fig. S5b).

Mutations of highly conserved amino acid residues reveal functional similarities and differences of SLC26A1

The congenital chloride-losing diarrhea mutation SLC26A3^{E293Q} and the paralogous engineered mutations SLC26A4^{E303Q}, SLC26A2^{E336Q}, and SLC26A6^{E298Q} exhibited loss-of-function in *Xenopus* oocytes without decrease in apparent surface expression [31,63]. The corresponding SLC26A1 mutant SLC26A1E295Q also exhibited 50% reduction of $^{35}SO_4^{2-}$ influx (Fig. 11a), but no reduction of $^{36}Cl^-$ influx (Fig. 11b) or of apparent SLC26A1surface expression.

In chicken SLC26A5/prestin, residues S398 and R399 have been proposed as substrate-binding sites, since mutation of these residues strongly disrupted prestin transport function [27]. Expression in oocytes of the corresponding mutant SLC26A1A400C reduced SLC26A1-mediated $^{35}SO_4^{2-}$ uptake by only 25% in ND96(Cl^-), and not at all in ND96(gluconate). Remarkably, $^{36}Cl^-$ influx into oocytes expressing mutant SLC26A1^{A400C} was unaffected. However, the adjacent corresponding mutant SLC26A1^{K401E} (corresponding to cPrestin R399) exhibited complete loss-of-function in uptake assays of $^{35}SO_4^{2-}$ and of $^{36}Cl^-$ (Fig. 11a,b). Neither putative anion substrate binding site mutant of human SLC26A1 exhibited reduced polypeptide abundance at or near the oocyte surface (Fig. 11c), suggesting preservation of overall transporter structure despite loss-of-function. HA-tagged SLC26A1 wildtype and mutant polypeptides showed similar results (data not shown).

SLC26A1 variants in the exome of a patient with recessive renal Fanconi syndrome do not confer loss-of-function

Inherited compound heterozygous variants SLC26A1^{C41W} and SLC26A1^{A56T} were found in the exome of a single Mexican child with recessive proximal tubular (PT) Fanconi Syndrome (~30x at ~80% coverage) in which mutations in Fanconi Syndrome gene NaPiIIa/SLC34A1 [47], and Fanconi-Bickel syndrome gene GLUT2/SLC5A2 [68] were not found. Both SLC26A1 variants were rare, with dbSNP-reported minor allele frequencies for C41W (rs43974931) of <0.5% and for A56T (rs142573758) of 0.02% . The C41W variant is predicted as "damaging" (SIFT) or "probably damaging" (Polyphen2). The A56T variant is predicted as "damaging" (SIFT) or "benign" (Polyphen2). The above characteristics and the shared basolateral proximal tubular localization of SLC26A1 with GLUT2 led to evaluation of the patient's SLC26A1 variants as candidate Fanconi Syndrome genes. Both $^{35}SO_4^{2-}$ uptake and ^{14}C-oxalate uptake mediated by SLC26A1^{C41W} in ND96(Cl^-) were normal or slightly elevated (Fig. 12a,b). $^{35}SO_4^{2-}$ uptake by SLC26A1A56T was also normal, and ^{14}C-oxalate uptake was minimally decreased (Fig. 12a,b). Interestingly, $^{36}Cl^-$ uptake associated with expression of either variant was substantially increased (Fig. 12c), as was (nominal) surface abundance of variant polypeptide (Fig. 12d,e). However, such a gain-of-function disease mutation would likely show a dominant inheritance pattern, incompatible with the reported good health of the heterozygous parent. In addition, the hypothetical contribution of SLC26A1 A56T to proximal tubular basolateral membrane Cl^- permeability [2,59,81] (if indeed electroneutral) should not decrease transepithelial reabsorption of HCO_3^-, glucose, or phosphate. Thus, the available functional data from expression in *Xenopus* oocytes do not support *SLC26A1* as the renal Fanconi Syndrome disease gene in this family.

SLC26A1 variants reported in a patient with nephrocalcinosis do not exhibit altered function

The rare heterozygous SLC26A1 variant SLC26A1^{M132T} was found *in trans* with the homozygous common variant Q566R in a patient with severe nephrocalcinosis requiring nephrectomy [19]. Since residue M132 is highly conserved across species orthologs, and the M132T-encoding variant is absent from dbSNP and predicted to be pathogenic, we subjected SLC26A1^{M132T} to functional testing in *Xenopus* oocytes, in isolation and *in cis* with common variant Q556R. We also coexpressed cRNAs encoding the double mutant with that encoding Q566R alone, to mimic the reported patient genotype. However, neither $^{35}SO_4^{2-}$ uptake from ND96(Cl^-) or from ND96(gluconate) nor ^{14}C-oxalate uptake from ND96(Cl^-) was reduced in oocytes expressing SLC26A1^{M132T} in any of the combinations tested (Fig. 13), suggesting that variant SLC26A1^{M132T} did not cause nephrolithiasis in this patient.

Discussion

Prompted by our preliminary identification of SLC26A1 as a candidate gene in a case of recessive renal Fanconi Syndrome, we conducted a comprehensive functional characterization of recombinant human SLC26A1 using the *Xenopus* oocyte heterologous expression system. SLC26A1-mediated $^{35}SO_4^{2-}/SO_4^{2-}$ exchange was DIDS-sensitive, apparently electroneutral, stimulated by alkaline pH_o and inhibited by acid pH_o, but was not regulated by acid pH_i over the pH range tested. SLC26A1-mediated $^{35}SO_4^{2-}$ uptake was almost completely dependent upon extracellular Cl^-, with $K_{1/2}$ for Cl^- cis-stimulation of 8-13 mM. The Cl^--stimulatory effect was mediated entirely by increasing V_{max} for SO_4^{2-} without altering $K_{1/2}$. The increased V_{max} reflected a dramatic, $Cl^-_{[o]}$-dependent decrease in sensitivity of SLC26A1-mediated SO_4^{2-} transport to inhibition by acid pH_o. $Cl^-_{[o]}$ was the most effective among other extracellular anions that also conferred cis-stimulation of SLC26A1-mediated SO_4^{2-}/SO_4^{2-} exchange.. SLC26A1-associated $^{36}Cl^-$ transport, unlike $^{35}SO_4^{2-}$ transport, was activated by acid pH_o and partially cation-dependent. The Na^+-dependent component of Cl^- transport was DIDS-sensitive, but insensitive to inhibitors of cation chloride cotransport. Table 1 summarizes the major differences observed between human SLC26A1-mediated $^{35}SO_4^{2-}$ transport and SLC26A1-associated Cl^- transport.

SLC26A1 also mediated 14C-oxalate uptake and $SO_4^{2-}{}_{[i]}$ /oxalate$_{[o]}$ exchange, but oxalate efflux in exchange for bath SO_4^{2-} (14C-oxalate$_{[i]}$/SO42-$_{[o]}$ exchange) was not detectable. SLC26A1 mediated SO_4^{2-} efflux in exchange for bath HCO_3-($^{35}SO_4^{2-}{}_{[i]}/HCO_3$-$_{[o]}$ exchange) and for bath thiosulfate ($^{35}SO_4^{2-}{}_{[i]}$/thiosulfate$_{[o]}$ exchange), but not in exchange for bath glyoxylate.

Mutation of residues corresponding to those crucial for SO_4^{2-} transport by chicken prestin/SLC26A5 altered SLC26A1-mediated $^{35}SO_4^{2-}$ transport in ways similar, but not identical to those in prestin. However, neither SLC26A1 missense variants found in a complete Fanconi syndrome patient nor different variants previously associated with nephrolithiasis/nephrocalcinosis exhibited loss-of-function phenotypes consistent with pathogenicity.

SLC26A1-mediated SO_4^{2-} transport

Our determination of 0.26 mM for $K_{1/2}$ of human SLC26A1-mediated SO_4^{2-} uptake (Fig. 1) is similar to those previously reported for rat (0.14 mM, [7]), and reported as data not shown for mouse (0.31 mM, [42]) and human SLC26A1 (0.19 mM, [61]). The human $K_{1/2}$ value is appropriate for a baso-lateral epithelial transporter in the presence of serum SO_4^{2-} concentrations of ~0.25-0.41 mM [50] that can double in late gestation [17] and triple during renal insufficiency [52]. Krick et al [40] previously characterized $K_{1/2}$ values for cis-inhibition of rat SLC26A1-mediated SO_4^{2-} uptake by extracellular HCO_3^-, thiosulfate, sulfite, and oxalate. As we observed for human SLC26A1 (Fig. S1), rat SLC26A1 function appeared electroneutral in Cl^- bath in both absence and presence of added SO_4^{2-} [40]. The related SO_4^{2-} transporter SLC26A2 was also shown to mediate electroneutral anion exchange [55].

pH-sensitivity of SLC26A1-mediated SO_4^{2-} transport

Acid pH_o inhibited and alkaline pH_o stimulated both influx and efflux of SO_4^{2-} by human SLC26A1 (Fig. 2). In marked contrast, SO_4^{2-} uptake by mouse SLC26A1 was stimulated by acid pH_o [82], and rat SLC26A1-mediated SO_4^{2-} uptake was inhibited by alkaline pH_o [40]. Human SLC26A1-mediated $SO_4^{2-}{}_{[i]}/OH^-{}_{[o]}$ exchange might account for part of the $^{35}SO_4^{2-}$ efflux stimulated by alkaline pH_o, but alkaline pH_o–stimulated SO_4^{2-} influx is less easily explained by $SO_4^{2-}[o]/OH^-{}_{[i]}$ exchange. The qualitatively identical regulatory effects of pH_o on both influx and efflux of SO_4^{2-} together suggest an allosteric regulatory effect of SO_4^{2-} transport. In the absence of pH_i-sensitive SO_4^{2-} transport by human SLC26A1, it is not straightforward to link the transporter's pH_o sensitivity to alkaline pH-stimulated proteoglycan sulfation [20] or to alkaline pH-stimulated metabolic N-sulfation of drugs [33]. We suggest that aa sequence differences in ecto-loops or elsewhere may explain the opposite pH-sensitivites of human and rodent SLC26A1.

$Cl^-_{[o]}$ regulates SLC26A1-mediated SO_4^{2-} transport by allosteric control of pH_o sensitivity

Human SLC26A1-mediated influx and efflux of SO_4^{2-} were stimulated greatly by $Cl^-_{[o]}$, and to comparable or lesser degrees by other extracellular anions tested (Fig. 4a,b; Supp. Fig. 4). $Cl^-_{[o]}$ exhibited cis-stimulation of $^{35}SO_4^{2-}$ uptake with Cl^- $K_{1/2}$ of ~8-13 mM (Fig. 3). $Cl^-_{[o]}$-mediated cis-stimulation of SO_4^{2-} uptake has also been noted as a property of SLC26A1 from mouse [82], eel [51], and rat [69]. However, $Cl^-_{[o]}$ did not stimulate human SLC26A1-mediated $^{35}SO_4^{2-}{}_{[i]}/Cl^-_{[o]}$ exchange in the complete absence of $SO_4^{2-}{}_{[o]}$ (Fig. 3e,f).

Bath Cl^- cis-stimulated $^{35}SO_4^{2-}$ uptake via increased Vmax without effect on $K_{1/2}$ for extracellular anion. The cis-stimulation reflected not a true V_{max} increase but rather a ~2 log shift of the pH_o vs. SO_4^{2-} uptake curve towards acid pH_o by bath Cl^- as compared to bath gluconate, and likely represents allosteric regulation by bath anion. The related SO_4^{2-} transporter SLC26A2 is also allosterically regulated by $Cl^-_{[o]}$, but by a mechanism (or utilizing a regulatory site of different anion affinity relative to the transport site) that co-exists with (the more frequently observed) cis-inhibition of SO_4^{2-} uptake by $Cl^-_{[o]}$. Stimulation by $Cl^-_{[o]}$ of mouse SLC26A2-mediated $SO_4^{2-}{}_{[i]}/OH^-{}_{[o]}$ exchange (monitored

by intracellular pH electrode) exhibited $Cl^-_{[o]}$ $K_{1/2}$ of ~4-8 mM [55], values similar to those reported here for human SLC26A1.

The aa residues constituting the regulatory binding site for Cl^- and other anions in SLC26A1 and SLC26A2 remain to be defined. Fluoride ion was reported (as data not shown) to inhibit the allosteric regulatory effect of $Cl^-_{[o]}$ on SLC26A2 [55]. $Cl^-_{[o]}$ has also been reported to regulate Cl^-/HCO_3-selectivity of CFTR in *Xenopus* oocytes [72], either directly via pore-widening [35] or via WNK kinase regulation [58]. The possible influences of these or related pathways on human SLC26A1 are unknown. Intracellular Cl^- regulatory sites with the GXXXP motif have been defined in SLC4A4/NBCe1-B [73], but a role for $Cl^-_{[i]}$ in regulation of SO_4^{2-} transport by SLC26A1 remains to undefined.

Regulation by $Cl^-_{[o]}$ with $K_{1/2}$ ~10 mM can be physiologically meaningful for an apical anion exchanger (such as SLC26A2) facing a low-Cl^- lumen [29]. However, understanding of such regulation is more challenging for a basolateral transporter such as SLC26A1 in proximal tubule and enterocytes exposed to interstitial fluid, for which a yet undefined anion, active in the presence of saturating Cl^-, may be a more potent physiological ligand of the regulatory ecto-site. Recently, SLC26A1 has been localized to the apical membrane in maturation phase ameloblasts in developing teeth of rat [85], a context in which physiological regulation by $Cl^-_{[o]}$ might occur. Alternatively, the regulatory ecto-binding site might be an evolutionary legacy from ancestral SLC26 genes or the conditions in which they functioned.

Transport of oxalate and other anions

SLC26A1 from mouse [82] and rat [40] was previously shown to take up oxalate. Ethylene glycol-induced hyperoxaluria in female (but not male) rats was accompanied by elevated hepatic and renal levels of SLC26A1 polypeptide, but not mRNA [10]. Human SLC26A1 displayed oxalate influx higher in $Cl^-_{[o]}$ than in baths of gluconate or cyclamate. Human SLC26A1 mediated DIDS-sensitive $^{35}SO_4^{2-}{}_{[i]}/oxalate_{[o]}$ exchange, but neither 14C-$oxalate_{[i]}/Cl^-_{[o]}$ exchange nor 14C-$oxalate_{[i]}/SO_4^{2-}{}_{[o]}$ exchange was detected (Fig. 5). This preferentially vectorial oxalate transport is consistent with the hypothesis that basolateral oxalate uptake by enterocytes is mediated by SLC26A1 as part of a transepithelial pathway that includes apical oxalate secretion into the gut lumen by SLC26A6 [18,49]. The macroscopically unidirectional transport may reflect a very low affinity of SLC26A1 for intracellular oxalate, or much higher affinities for other coextant substrate anions at the intracellular substrate binding site. However, such a system is not active throughout the gut, as evidenced by normal *ex vivo* oxalate secretion rates by the isolated *SLC26A1*$^{-/-}$ mouse duodenum [39].

Human SLC26A1 exchange of $SO_4^{2-}{}_{[i]}$ for bath HCO_3- and bath thiosulfate (Fig. 6a-d) resembled that of rat SLC26A1 [40]. Thus, SLC26A1 may play a role in the action of exogenous thiosulfate in treatment or prophylaxis of calciphylaxis [54,57] and possibly also in the metabolism of H_2S, both a precursor of endogenous thiosulfate and a product of exogenous thiosulfate [43]. Unlike rat SLC26A1 [70], recombinant human SLC26A1 did not exhibit glyoxylate transport (Fig. 6e-g), despite the ability of chronic glyoxylate exposure to increase SLC26A1 mRNA and SO_4^{2-} uptake in human HepG2 cells [70]. Thus,

our *Xenopus* oocyte data do not support the otherwise attractive model of hepatic SLC26A1-mediated glyoxylate/oxalate exchange proposed by Schnedler et al. [70].

Transport of Cl^- associated with SLC26A1 expression in Xenopus oocytes

Human SLC26A1 mediated robust uptake of Cl^- which is increased further by acid pH_o (Fig. 7a), in contrast to inhibition of human SLC26A1-mediated SO_4^{2-} transport by acid pH_o (Fig. 2). SLC26A1-mediated Cl^- efflux into Cl^- bath or gluconate bath was also increased by acid pH_o, results not consistent with SLC26A1-mediated $Cl^-_{[i]}/OH^-_{[o]}$ exchange. These results also differed from alkaline pH_o stimulation of SO_4^{2-} efflux, consistent with SLC26A1-mediated $^{35}SO_4^{2-}{}_{[i]}/OH^-_{[o]}$ exchange. SLC26A1-associated $36Cl^-$ efflux into baths of Cl^- or gluconate were of lower rate and lower DIDS-sensitivity than was the case for SLC26A1-mediated SO_4^{2-} transport (Fig. 8). Among other SLC26 polypeptides, acid pH_o also increased SLC26A9-mediated Cl^- currents [22,65].

Unlike the Na+-independence of SLC26A1-mediated SO_4^{2-} transport, SLC26A1-associated Cl^- flux displayed partial Na^+-dependence (Fig. 9). $NMDG^+$ substitution of bath Na^+ abolished the DIDS-sensitive component of Cl^- flux. SLC26A1-mediated Cl^- uptake was insensitive to inhibition by cation-Cl^- cotransporter blockers and to niflumate. Although K^+ substitution of bath Na^+ did not reduce Cl^- uptake, its DIDS-sensitive component was abolished, suggesting that high bath K^+ activated a DIDS-insensitive, SLC26A1-dependent Cl^- uptake. The reported Na^+-dependent component of SLC26A9-mediated Cl^- transport was DIDS-sensitive [46,67] and represented (at least in part) coupled transport of Na^+ with Cl^- [13], albeit insensitive to inhibitors of cation chloride cotransport. The previously reported lack of Cl^- transport by mouse SLC26A1 [82] was based on experiments carried out in Na^+-free, $NMDG^+$ solutions. In contrast, the previous report of Cl^- transport associated with human SLC26A1 expression [61] reflected experiments carried out in Na gluconate bath.

Protein Kinase C (PKC) regulation of SLC26A1

PKC activation by PMA was first shown to downregulate SLC26A6 activity through decreased cell surface expression, and pharmacological approaches suggested regulation by PKCδ [30]. Documentation of inhibition by PMA-mediated activation of PKC was extended to SLC26A2 [31] and SLC26A3, but SLC26A4 was unaffected by PMA. Activated PKCδ was more definitively implicated as inhibitor of SLC26A2, -A3, and -A6 through attenuation of inhibition by co-expressed kinase-dead PKCδ [64]. Here we have demonstrated PMA-mediated inhibition of SLC26A1 by a mechanism other than regulation of surface expression (Fig. 10). This PMA response may reflect involvement of a different PKC isoform. Further work will determine whether SLC26A1 inhibition by PMA is mediated via direct phosphorylation or requires intermediate signaling steps.

Divergent effects of SLC26A1 mutations on transport of SO_4^{2-} and Cl^-

The structural fold of paralogous SLC26 proteins accommodates anion exchangers of varied selectivity and mechanism, anion channels, and proteins with apparent plasticity of anion selectivity and mechanism [1,74]. Therefore, the functional consequences of mutation in selected residues previously shown crucial for anion transport activity in other SLC26 family

members were tested in SLC26A1. Human SLC26A3 disease mutant E293Q exhibited loss of $^{36}Cl^-$/anion exchange function without decrease in surface expression [64]. The corresponding human SLC26A1mutant E295Q showed partial reduction of $^{35}SO_4^{2-}$ transport without reduction in either $36Cl^-$ transport or polypeptide surface expression, highlighting differences between SO_4^{2-} and Cl^- transport by SLC26A1.

Chicken prestin and human SLC26A1 both mediate SO_4^{2-}/oxalate exchange, but prestin can also mediate electrogenic Cl^-/oxalate and Cl^-/SO_4^{2-} exchange. Mutations in candidate anion substrate binding site residue R405 in the inner anion translocation pathway of chicken prestin/SLC26A5 completely abolished anion transport, and the corresponding mutation R399C in rat prestin abolished anion-dependent non-linear capacitance [27]. The corresponding SLC26A1 mutant K401E completely abolished transport of $^{35}SO_4^{2-}$ in the presence of either bath Cl^- or gluconate, and abolished $36Cl^-$ transport, as well. The adjacent SLC26A1 mutation A400C partially reduced $^{35}SO_4^{2-}$ transport only in the presence of bath Cl^-, but not gluconate, and was without effect on SLC26A1-mediated $^{36}Cl^-$ uptake. Thus residues defined by mutagenesis as important for anion exchange by chicken prestin/SLC26A5 are also important for anion exchange by SLC26A1, but the mutations studied differentially affect SLC26A1-mediated transport of SO_4^{2-} and of Cl^-. This difference may reflect, at least in part, a contribution of endogenous oocyte Cl^- transport pathways activated by recombinant expression of SLC26A1.

Xenopus oocyte functional expression data suggest that the SLC26A1 variants identified in a patient with renal Fanconi Syndrome and a patient with nephrolithiasis-calcinosis do not contribute to pathogenesis of these conditions

SLC26A1 variants found in a patient with Fanconi Syndrome exhibited no decrease in transport of either SO_4^{2-}, oxalate, or Cl^- (Fig. 12). Indeed, the C41W variant increased transport of both Cl^- and SO_4^{2-} without change in oocyte surface expression. In contrast, variant A56T increased Cl^- transport by 4-fold but slightly decreased oxalate transport, both in parallel with 4-fold 65% increased polypeptide expression at or near the oocyte surface. These functional properties do not suggest a causative role for these SLC26A1 mutants in renal Fanconi syndrome.

The rare heterozygous SLC26A1 variant M132T and the common homozygous variant Q556R, found together in a patient with recurrent nephrolithiasis and nephrocalcinosis [19], did not alter transport of SO_4^{2-} or oxalate, whether expressed individually or co-expressed (Fig. 13). Thus, the functional properties of these variants expressed in *Xenopus* oocytes do not suffice to explain nephrolithiasis or nephrocalcinosis in this patient. We cannot rule out the possibility that detection of impaired trafficking, or transport phenotypes of either the Fanconi variants or the nephrolithiasis/ calcinosis variants of SLC26A1 might require expression inpolarized mammalian epithelial cells that express yet unidentified interaction partners of SLC26A1. Nonetheless, as a basolateral oxalate uptake mechanism of intestinal and proximal tubular epithelial cells, inclusion of the *SLC26A1* gene in genetic variant screens of nephrolithiasis/calcinosis patients is reasonable.

Conclusion

The functional properties of human SLC26A1 emphasize the context-dependent functional complexity among not only paralogs but even species orthologs of SLC26 anion transporter polypeptides. Although human SLC26A1 shared with its paralogs the ability to mediate apparently electroneutral, cis-Cl^--stimulated exchange of sulfate and oxalate, and transport of bicarbonate and thiosulfate, it differed from those paralogs in several notable ways. Human SLC26A1 exhibited pH-dependent sulfate exchange that was opposite to that of rodent SLC26A1, as well as opposite to that exhibited by human SLC26A1-associated Cl^- transport. Human SLC26A1 differed from rat SLC26A1 in its inability to mediate oxalate/glyoxalate exchange. Human SLC26A1 exhibited partial and limited cation-dependence of its substantial associated Cl^- uptake. In contrast to other human SLC26 anion exchangers, human SLC26A1 inhibition by PKC was unassociated with decreased polypeptide expression at or near the oocyte surface.

The major mechanistic finding presented here is the demonstration that the cis-stimulation of human SLC26A1-mediated anion exchange by $Cl^-_{[o]}$ is a V_{max} effect mediated by allosteric regulation of the transporter's pH_o-sensitivity. The recently published crystal structure of the TMD of bacterial SulP/SLC26 multi-anion transporter SLC26Dg [24], and the confirmation of its previously suspected contextual modulation of anion selectivity [3,24,74] will aid in the structural analysis of allosteric regulatory interplay extracellular protons and anions in the control of human SLC26A1 activity.

Supplementary Material

Refer to Web version on PubMed Central for supplementary material.

Acknowledgements

The authors thank Norma Guerra, MD (Hospital IMSS la Raza, Ciudad de Mexico, Mexico) for patient samples.

References

1. Alper SL, Sharma AK. The SLC26 gene family of anion transporters and channels. Molecular aspects of medicine. 2013; 34:494–515. doi:10.1016/j.mam.2012.07.009. [PubMed: 23506885]
2. Aronson PS, Giebisch G. Mechanisms of chloride transport in the proximal tubule. The American journal of physiology. 1997; 273:F179–192. [PubMed: 9277578]
3. Babu M, Greenblatt JF, Emili A, Strynadka NC, Reithmeier RA, Moraes TF. Structure of a SLC26 anion transporter STAS domain in complex with acyl carrier protein: implications for E. coli YchM in fatty acid metabolism. Structure (London, England : 1993). 2010; 18:1450–1462. doi:10.1016/j.str.2010.08.015.
4. Barbosa M, Sousa AB, Medeira A, Lourenco T, Saraiva J, Pinto-Basto J, Soares G, Fortuna AM, Superti-Furga A, Mittaz L, Reis-Lima M, Bonafe L. Clinical and molecular characterization of Diastrophic Dysplasia in the Portuguese population. Clinical genetics. 2011; 80:550–557. doi:10.1111/j.1399-0004.2010.01595.x. [PubMed: 21155763]
5. Bian S, Navaratnam D, Santos-Sacchi J. Real time measures of prestin charge and fluorescence during plasma membrane trafficking reveal sub-tetrameric activity. PloS one. 2013; 8:e66078. doi:10.1371/journal.pone.0066078. [PubMed: 23762468]
6. Biber J, Murer H, Mohebbi N, Wagner CA. Renal handling of phosphate and sulfate. Comprehensive Physiology. 2014; 4:771–792. doi:10.1002/cphy.c120031. [PubMed: 24715567]

7. Bissig M, Hagenbuch B, Stieger B, Koller T, Meier PJ. Functional expression cloning of the canalicular sulfate transport system of rat hepatocytes. The Journal of biological chemistry. 1994; 269:3017–3021. [PubMed: 8300633]
8. Bizhanova A, Kopp P. Genetics and phenomics of Pendred syndrome. Molecular and cellular endocrinology. 2010; 322:83–90. doi:10.1016/j.mce.2010.03.006. [PubMed: 20298745]
9. Blackman SM, Commander CW, Watson C, Arcara KM, Strug LJ, Stonebraker JR, Wright FA, Rommens JM, Sun L, Pace RG, Norris SA, Durie PR, Drumm ML, Knowles MR, Cutting GR. Genetic modifiers of cystic fibrosis-related diabetes. Diabetes. 2013; 62:3627–3635. doi:10.2337/db13-0510. [PubMed: 23670970]
10. Breljak D, Brzica H, Vrhovac I, Micek V, Karaica D, Ljubojevic M, Sekovanic A, Jurasovic J, Rasic D, Peraica M, Lovric M, Schnedler N, Henjakovic M, Wegner W, Burckhardt G, Burckhardt BC, Sabolic I. In female rats, ethylene glycol treatment elevates protein expression of hepatic and renal oxalate transporter sat-1 (Slc26a1) without inducing hyperoxaluria. Croatian medical journal. 2015; 56:447–459. [PubMed: 26526882]
11. Brzica H, Breljak D, Burckhardt BC, Burckhardt G, Sabolic I. Oxalate: from the environment to kidney stones. Arhiv za higijenu rada i toksikologiju. 2013; 64:609–630. doi:10.2478/10004-1254-64-2013-2428. [PubMed: 24384768]
12. Brzica H, Breljak D, Krick W, Lovric M, Burckhardt G, Burckhardt BC, Sabolic I. The liver and kidney expression of sulfate anion transporter sat-1 in rats exhibits male-dominant gender differences. Pflugers Archiv : European journal of physiology. 2009; 457:1381–1392. doi:10.1007/s00424-008-0611-5. [PubMed: 19002488]
13. Chang MH, Plata C, Zandi-Nejad K, Sindic A, Sussman CR, Mercado A, Broumand V, Raghuram V, Mount DB, Romero MF. Slc26a9--anion exchanger, channel and Na+ transporter. The Journal of membrane biology. 2009; 228:125–140. doi:10.1007/s00232-009-9165-5. [PubMed: 19365592]
14. Compton EL, Karinou E, Naismith JH, Gabel F, Javelle A. Low resolution structure of a bacterial SLC26 transporter reveals dimeric stoichiometry and mobile intracellular domains. The Journal of biological chemistry. 2011; 286:27058–27067. doi:10.1074/jbc.M111.244533. [PubMed: 21659513]
15. Cordat E, Reithmeier RA. Structure, function, and trafficking of SLC4 and SLC26 anion transporters. Current topics in membranes. 2014; 73:1–67. doi:10.1016/b978-0-12-800223-0.00001-3. [PubMed: 24745980]
16. Dawson PA. Sulfate in fetal development. Seminars in cell & developmental biology. 2011; 22:653–659. doi:10.1016/j.semcdb.2011.03.004. [PubMed: 21419855]
17. Dawson PA, Elliott A, Bowling FG. Sulphate in pregnancy. Nutrients. 2015; 7:1594–1606. doi:10.3390/nu7031594. [PubMed: 25746011]
18. Dawson PA, Russell CS, Lee S, McLeay SC, van Dongen JM, Cowley DM, Clarke LA, Markovich D. Urolithiasis and hepatotoxicity are linked to the anion transporter Sat1 in mice. The Journal of clinical investigation. 2010; 120:706–712. doi:10.1172/jci31474. [PubMed: 20160351]
19. Dawson PA, Sim P, Mudge DW, Cowley D. Human SLC26A1 gene variants: a pilot study. TheScientificWorldJournal. 20132013:541710. doi:10.1155/2013/541710.
20. Dick G, Akslen-Hoel LK, Grondahl F, Kjos I, Prydz K. Proteoglycan synthesis and Golgi organization in polarized epithelial cells. The journal of histochemistry and cytochemistry : official journal of the Histochemistry Society. 2012; 60:926–935. doi:10.1369/0022155412461256. [PubMed: 22941419]
21. Dirami T, Rode B, Jollivet M, Da Silva N, Escalier D, Gaitch N, Norez C, Tuffery P, Wolf JP, Becq F, Ray PF, Dulioust E, Gacon G, Bienvenu T, Toure A. Missense mutations in SLC26A8, encoding a sperm-specific activator of CFTR, are associated with human asthenozoospermia. American journal of human genetics. 2013; 92:760–766. doi:10.1016/j.ajhg.2013.03.016. [PubMed: 23582645]
22. Romero, MF.; Chang, MH.; Plata, C.; Zandi-Nejad, K.; Mercado, A.; Broumand, V.; Sussman, CR.; Mount, DB. Epithelial Anion Transport in Health and Disease: the Role of the SLC26 Transport Family. Vol. 273. Novartis Foundation Symposium; 2006. Physiology of electrogenic SLC26 paralogs; p. 126-147.

23. Freel RW, Hatch M. Hyperoxaluric rats do not exhibit alterations in renal expression patterns of Slc26a1 (SAT1) mRNA or protein. Urological research. 2012; 40:647–654. doi:10.1007/s00240-012-0480-4. [PubMed: 22573180]
24. Geertsma ER, Chang YN, Shaik FR, Neldner Y, Pardon E, Steyaert J, Dutzler R. Structure of a prokaryotic fumarate transporter reveals the architecture of the SLC26 family. Nature structural & molecular biology. 2015; 22:803–808. doi:10.1038/nsmb.3091.
25. Glatt H, Meinl W. Pharmacogenetics of soluble sulfotransferases (SULTs). Naunyn-Schmiedeberg's archives of pharmacology. 2004; 369:55–68. doi:10.1007/s00210-003-0826-0.
26. Good NE, Winget GD, Winter W, Connolly TN, Izawa S, Singh RM. Hydrogen ion buffers for biological research. Biochemistry. 1966; 5:467–477. [PubMed: 5942950]
27. Gorbunov D, Sturlese M, Nies F, Kluge M, Bellanda M, Battistutta R, Oliver D. Molecular architecture and the structural basis for anion interaction in prestin and SLC26 transporters. Nature communications. 2014; 5:3622. doi:10.1038/ncomms4622.
28. Habuchi H, Habuchi O, Kimata K. Sulfation pattern in glycosaminoglycan: does it have a code? Glycoconjugate journal. 2004; 21:47–52. doi:10.1023/B:GLYC.0000043747.87325.5e. [PubMed: 15467398]
29. Haila S, Hastbacka J, Bohling T, Karjalainen-Lindsberg ML, Kere J, Saarialho-Kere U. SLC26A2 (diastrophic dysplasia sulfate transporter) is expressed in developing and mature cartilage but also in other tissues and cell types. The journal of histochemistry and cytochemistry : official journal of the Histochemistry Society. 2001; 49:973–982. [PubMed: 11457925]
30. Hassan HA, Mentone S, Karniski LP, Rajendran VM, Aronson PS. Regulation of anion exchanger Slc26a6 by protein kinase C. American journal of physiology Cell physiology. 2007; 292:C1485–1492. doi:10.1152/ajpcell.00447.2006. [PubMed: 17151144]
31. Heneghan JF, Akhavein A, Salas MJ, Shmukler BE, Karniski LP, Vandorpe DH, Alper SL. Regulated transport of sulfate and oxalate by SLC26A2/DTDST. American journal of physiology Cell physiology. 2010; 298:C1363–1375. doi:10.1152/ajpcell.00004.2010. [PubMed: 20219950]
32. Hierholzer K, Cade R, Gurd R, Kessler R, Pitts R. Stop-flow analysis of renal reabsorption and excretion of sulfate in the dog. The American journal of physiology. 1960; 198:833–837. [PubMed: 14401728]
33. Jia C, Luo L, Kurogi K, Yu J, Zhou C, Liu MC. Identification of the human SULT enzymes involved in the metabolism of rotigotine. Journal of clinical pharmacology. 2015 doi:10.1002/jcph.658.
34. Jiang Z, Asplin JR, Evan AP, Rajendran VM, Velazquez H, Nottoli TP, Binder HJ, Aronson PS. Calcium oxalate urolithiasis in mice lacking anion transporter Slc26a6. Nature genetics. 2006; 38:474–478. doi:10.1038/ng1762. [PubMed: 16532010]
35. Jun I, Cheng MH, Sim E, Jung J, Suh BL, Kim Y, Son H, Park K, Kim CH, Yoon JH, Whitcomb DC, Bahar I, Lee MG. Pore dilation increases the bicarbonate permeability of CFTR, ANO1, and glycine receptor anion channels. The Journal of physiology. 2015 doi:10.1113/jp271311.
36. Karinou E, Compton EL, Morel M, Javelle A. The Escherichia coli SLC26 homologue YchM (DauA) is a C(4)-dicarboxylic acid transporter. Molecular microbiology. 2013; 87:623–640. doi:10.1111/mmi.12120. [PubMed: 23278959]
37. Karniski LP, Lotscher M, Fucentese M, Hilfiker H, Biber J, Murer H. Immunolocalization of sat-1 sulfate/oxalate/bicarbonate anion exchanger in the rat kidney. The American journal of physiology. 1998; 275:F79–87. [PubMed: 9689008]
38. Knight TF, Sansom SC, Senekjian HO, Weinman EJ. Oxalate secretion in the rat proximal tubule. The American journal of physiology. 1981; 240:F295–298. [PubMed: 7223887]
39. Ko N, Knauf F, Jiang Z, Markovich D, Aronson PS. Sat1 is dispensable for active oxalate secretion in mouse duodenum. American journal of physiology Cell physiology. 2012; 303:C52–57. doi:10.1152/ajpcell.00385.2011. [PubMed: 22517357]
40. Krick W, Schnedler N, Burckhardt G, Burckhardt BC. Ability of sat-1 to transport sulfate, bicarbonate, or oxalate under physiological conditions. American journal of physiology Renal physiology. 2009; 297:F145–154. doi:10.1152/ajprenal.90401.2008. [PubMed: 19369292]

41. Kuo SM, Aronson PS. Oxalate transport via the sulfate/HCO3 exchanger in rabbit renal basolateral membrane vesicles. The Journal of biological chemistry. 1988; 263:9710–9717. [PubMed: 3384817]
42. Lee A, Beck L, Markovich D. The mouse sulfate anion transporter gene Sat1 (Slc26a1): cloning, tissue distribution, gene structure, functional characterization, and transcriptional regulation thyroid hormone. DNA and cell biology. 2003; 22:19–31. doi:10.1089/104454903321112460. [PubMed: 12590734]
43. Levitt MD, Furne J, Springfield J, Suarez F, DeMaster E. Detoxification of hydrogen sulfide and methanethiol in the cecal mucosa. The Journal of clinical investigation. 1999; 104:1107–1114. doi: 10.1172/jci7712. [PubMed: 10525049]
44. Li J, Xia F, Reithmeier RA. N-glycosylation and topology of the human SLC26 family of anion transport membrane proteins. American journal of physiology Cell physiology. 2014; 306:C943–960. doi:10.1152/ajpcell.00030.2014. [PubMed: 24647542]
45. Liu XZ, Ouyang XM, Xia XJ, Zheng J, Pandya A, Li F, Du LL, Welch KO, Petit C, Smith RJH, Webb BT, Yan D, Arnos KS, Corey D, Dallos P, Nance WE, Chen ZY. Prestin, a cochlear motor protein, is defective in non-syndromic hearing loss. Human Molecular Genetics. 2003; 12:1155–1162. doi:10.1093/hmg/ddg127. [PubMed: 12719379]
46. Loriol C, Dulong S, Avella M, Gabillat N, Boulukos K, Borgese F, Ehrenfeld J. Characterization of SLC26A9, facilitation of Cl(-) transport by bicarbonate. Cellular physiology and biochemistry : international journal of experimental cellular physiology, biochemistry, and pharmacology. 2008; 22:15–30. doi:10.1159/000149780.
47. Magen D, Berger L, Coady MJ, Ilivitzki A, Militianu D, Tieder M, Selig S, Lapointe JY, Zelikovic I, Skorecki K. A loss-of-function mutation in NaPi-IIa and renal Fanconi's syndrome. The New England journal of medicine. 2010; 362:1102–1109. doi:10.1056/NEJMoa0905647. [PubMed: 20335586]
48. Markovich D. Physiological roles of renal anion transporters NaS1 and Sat1. American journal of physiology Renal physiology. 2011; 300:F1267–1270. doi:10.1152/ajprenal.00061.2011. [PubMed: 21490138]
49. Markovich D. Slc13a1 and Slc26a1 KO models reveal physiological roles of anion transporters. Physiology (Bethesda, Md). 2012; 27:7–14. doi:10.1152/physiol.00041.2011.
50. Morris ME, Levy G. Serum concentration and renal excretion by normal adults of inorganic sulfate after acetaminophen, ascorbic acid, or sodium sulfate. Clinical pharmacology and therapeutics. 1983; 33:529–536. [PubMed: 6831833]
51. Makada T, Zandi-Nejad K, Kurita Y, Kudo H, Broumand V, Kwon CY, Mercado A, Mount DB, Hirose S. Roles of Slc13a1 and Slc26a1 sulfate transporters of eel kidney in sulfate homeostasis and osmoregulation in freshwater. American journal of physiology Regulatory, integrative and comparative physiology. 2005; 289:R575–r585. doi:10.1152/ajpregu.00725.2004.
52. Makanishi T, Otaki Y, Hasuike Y, Nanami M, Itahana R, Miyagawa K, Nishikage H, Izumi M, Takamitsu Y. Association of hyperhomocysteinemia with plasma sulfate and urine sulfate excretion in patients with progressive renal disease. American journal of kidney diseases : the official journal of the National Kidney Foundation. 2002; 40:909–915. doi:10.1053/ajkd.2002.36320. [PubMed: 12407634]
53. Nazzal L, Puri S, Goldfarb DS. Enteric hyperoxaluria: an important cause of end-stage kidney disease. Nephrology, dialysis, transplantation : official publication of the European Dialysis and Transplant Association - European Renal Association. 2015 doi:10.1093/ndt/gfv005.
54. Nigwekar SU, Brunelli SM, Meade D, Wang W, Hymes J, Lacson E Jr. Sodium thiosulfate therapy for calcific uremic arteriolopathy. Clinical journal of the American Society of Nephrology : CJASN. 2013; 8:1162–1170. doi:10.2215/cjn.09880912. [PubMed: 23520041]
55. Ohana E, Shcheynikov N, Park M, Muallem S. Solute carrier family 26 member a2 (Slc26a2) protein functions as an electroneutral SOFormula/OH-/Cl^- exchanger regulated by extracellular Cl. The Journal of biological chemistry. 2012; 287:5122–5132. doi:10.1074/jbc.M111.297192. [PubMed: 22190686]
56. Ohana E, Yang D, Shcheynikov N, Muallem S. Diverse transport modes by the solute carrier 26 family of anion transporters. The Journal of physiology. 2009; 587:2179–2185. doi:10.1113/jphysiol.2008.164863. [PubMed: 19015189]

57. Okonkwo OW, Batwara R, Granja I, Asplin JR, Goldfarb DS. A pilot study of the effect of sodium thiosulfate on urinary lithogenicity and associated metabolic acid load in non-stone formers and stone formers with hypercalciuria. PloS one. 2013; 8:e60380. doi:10.1371/journal.pone.0060380. [PubMed: 23593205]
58. Park HW, Nam JH, Kim JY, Namkung W, Yoon JS, Lee JS, Kim KS, Venglovecz V, Gray MA, Kim KH, Lee MG. Dynamic regulation of CFTR bicarbonate permeability by [Cl⁻]i and its role in pancreatic bicarbonate secretion. Gastroenterology. 2010; 139:620–631. doi:10.1053/j.gastro.2010.04.004. [PubMed: 20398666]
59. Planelles G. Chloride transport in the renal proximal tubule. Pflugers Archiv : European journal of physiology. 2004; 448:561–570. doi:10.1007/s00424-004-1309-y. [PubMed: 15258765]
60. Quondamatteo F, Krick W, Hagos Y, Kruger MH, Neubauer-Saile K, Herken R, Ramadori G, Burckhardt G, Burckhardt BC. Localization of the sulfate/anion exchanger in the rat liver. American journal of physiology Gastrointestinal and liver physiology. 2006; 290:G1075–1081. doi:10.1152/ajpgi.00492.2005. [PubMed: 16357056]
61. Regeer RR, Lee A, Markovich D. Characterization of the human sulfate anion transporter (hsat-1) protein and gene (SAT1; SLC26A1). DNA and cell biology. 2003; 22:107–117. doi:10.1089/104454903321515913. [PubMed: 12713736]
62. Regeer RR, Markovich D. A dileucine motif targets the sulfate anion transporter sat-1 to the basolateral membrane in renal cell lines. American journal of physiology Cell physiology. 2004; 287:C365–372. doi:10.1152/ajpcell.00502.2003. [PubMed: 15070814]
63. Reimold FR, Balasubramanian S, Doroquez DB, Shmukler BE, Zsengeller ZK, Saslowsky D, Thiagarajah JR, Stillman IE, Lencer WI, Wu BL, Villalpando-Carrion S, Alper SL. Congenital chloride-losing diarrhea in a Mexican child with the novel homozygous SLC26A3 mutation G393W. Frontiers in physiology. 2015; 6:179. doi:10.3389/fphys.2015.00179. [PubMed: 26157392]
64. Reimold FR, Heneghan JF, Stewart AK, Zelikovic I, Vandorpe DH, Shmukler BE, Alper SL. Pendrin function and regulation in Xenopus oocytes. Cellular physiology and biochemistry : international journal of experimental cellular physiology, biochemistry, and pharmacology. 2011; 28:435–450. doi:10.1159/000335106.
65. Romero MF, Chang MH, Plata C, Zandi-Nejad K, Mercado A, Broumand V, Sussman CR, Mount DB. Physiology of electrogenic SLC26 paralogues. Novartis Foundation symposium. 2006; 273:126–138. discussion 138-147, 261-124. [PubMed: 17120765]
66. Rungta RL, Choi HB, Tyson JR, Malik A, Dissing-Olesen L, Lin PJ, Cain SM, Cullis PR, Snutch TP, MacVicar BA. The cellular mechanisms of neuronal swelling underlying cytotoxic edema. Cell. 2015; 161:610–621. doi:10.1016/j.cell.2015.03.029. [PubMed: 25910210]
67. Salomon JJ, Spahn S, Wang X, Fullekrug J, Bertrand CA, Mall MA. Generation and functional characterization of epithelial cells with stable expression of SLC26A9 Cl⁻ channels. American journal of physiology Lung cellular and molecular physiology:ajplung. 2016; 00321:02015. doi:10.1152/ajplung.00321.2015.
68. Santer R, Calado J. Familial renal glucosuria and SGLT2: from a mendelian trait to a therapeutic target. Clinical journal of the American Society of Nephrology : CJASN. 2010; 5:133–141. doi:10.2215/cjn.04010609. [PubMed: 19965550]
69. Satoh H, Susaki M, Shukunami C, Iyama K, Negoro T, Hiraki Y. Functional analysis of diastrophic dysplasia sulfate transporter. Its involvement in growth regulation of chondrocytes mediated by sulfated proteoglycans. The Journal of biological chemistry. 1998; 273:12307–12315. [PubMed: 9575183]
70. Schnedler N, Burckhardt G, Burckhardt BC. Glyoxylate is a substrate of the sulfate-oxalate exchanger, sat-1, and increases its expression in HepG2 cells. Journal of hepatology. 2011; 54:513–520. doi:10.1016/j.jhep.2010.07.036. [PubMed: 21093948]
71. Senekjian HO, Weinman EJ. Oxalate transport by proximal tubule of the rabbit kidney. The American journal of physiology. 1982; 243:F271–275. [PubMed: 7114257]
72. Shcheynikov N, Kim KH, Kim KM, Dorwart MR, Ko SB, Goto H, Naruse S, Thomas PJ, Muallem S. Dynamic control of cystic fibrosis transmembrane conductance regulator Cl(−)/HCO3(−) selectivity by external Cl(−). The Journal of biological chemistry. 2004; 279:21857–21865. doi:10.1074/jbc.M313323200. [PubMed: 15010471]

73. Shcheynikov N, Son A, Hong JH, Yamazaki O, Ohana E, Kurtz I, Shin DM, Muallem S. Intracellular Cl^- as a signaling ion that potently regulates Na+/HCO3-transporters. Proceedings of the National Academy of Sciences of the United States of America. 2015; 112:E329–337. doi: 10.1073/pnas.1415673112. [PubMed: 25561556]
74. Srinivasan L, Baars TL, Fendler K, Michel H. Functional characterization of solute carrier (SLC) 26/sulfate permease (SulP) proteins in membrane mimetic systems. Biochimica et biophysica acta. 2016; 1858:698–705. doi:10.1016/j.bbamem.2016.01.006. [PubMed: 26774215]
75. Stewart AK, Chernova MN, Kunes YZ, Alper SL. Regulation of AE2 anion exchanger by intracellular pH: critical regions of the NH(2)-terminal cytoplasmic domain. American journal of physiology Cell physiology. 2001; 281:C1344–1354. [PubMed: 11546673]
76. Subramanian VS, Nabokina SM, Patton JR, Marchant JS, Moradi H, Said HM. Glyoxalate reductase/hydroxypyruvate reductase interacts with the sodium-dependent vitamin C transporter-1 to regulate cellular vitamin C homeostasis. American journal of physiology Gastrointestinal and liver physiology. 2013; 304:G1079–1086. doi:10.1152/ajpgi.00090.2013. [PubMed: 23599041]
77. Sun L, Rommens JM, Corvol H, Li W, Li X, Chiang TA, Lin F, Dorfman R, Busson PF, Parekh RV, Zelenika D, Blackman SM, Corey M, Doshi VK, Henderson L, Naughton KM, O'Neal WK, Pace RG, Stonebraker JR, Wood SD, Wright FA, Zielenski J, Clement A, Drumm ML, Boelle PY, Cutting GR, Knowles MR, Durie PR, Strug LJ. Multiple apical plasma membrane constituents are associated with susceptibility to meconium ileus in individuals with cystic fibrosis. Nature genetics. 2012; 44:562–569. doi:10.1038/ng.2221. [PubMed: 22466613]
78. Wang X, Yang S, Jia S, He DZ. Prestin forms oligomer with four mechanically independent subunits. Brain research. 2010; 1333:28–35. doi:10.1016/j.brainres.2010.03.070. [PubMed: 20347723]
79. Wangemann P. Mouse models for pendrin-associated loss of cochlear and vestibular function. Cellular physiology and biochemistry : international journal of experimental cellular physiology, biochemistry, and pharmacology. 2013; 32:157–165. doi:10.1159/000356635.
80. Wedenoja S, Pekansaari E, Hoglund P, Makela S, Holmberg C, Kere J. Update on SLC26A3 mutations in congenital chloride diarrhea. Human mutation. 2011; 32:715–722. doi:10.1002/humu.21498. [PubMed: 21394828]
81. Weinstein AM, Weinbaum S, Duan Y, Du Z, Yan Q, Wang T. Flow-dependent transport in a mathematical model of rat proximal tubule. American journal of physiology Renal physiology. 2007; 292:F1164–1181. doi:10.1152/ajprenal.00392.2006. [PubMed: 17213461]
82. Xie Q, Welch R, Mercado A, Romero MF, Mount DB. Molecular characterization of the murine Slc26a6 anion exchanger: functional comparison with Slc26a1. American journal of physiology Renal physiology. 2002; 283:F826–838. doi:10.1152/ajprenal.00079.2002. [PubMed: 12217875]
83. Xu J, Song P, Miller ML, Borgese F, Barone S, Riederer B, Wang Z, Alper SL, Forte JG, Shull GE, Ehrenfeld J, Seidler U, Soleimani M. Deletion of the chloride transporter Slc26a9 causes loss of tubulovesicles in parietal cells and impairs acid secretion in the stomach. Proceedings of the National Academy of Sciences of the United States of America. 2008; 105:17955–17960. doi: 10.1073/pnas.0800616105. [PubMed: 19004773]
84. Xu J, Song P, Nakamura S, Miller M, Barone S, Alper SL, Riederer B, Bonhagen J, Arend LJ, Amlal H, Seidler U, Soleimani M. Deletion of the chloride transporter slc26a7 causes distal renal tubular acidosis and impairs gastric acid secretion. The Journal of biological chemistry. 2009; 284:29470–29479. doi:10.1074/jbc.M109.044396. [PubMed: 19723628]
85. Yin K, Lei Y, Wen X, Lacruz RS, Soleimani M, Kurtz I, Snead ML, White SN, Paine ML. SLC26A Gene Family Participate in pH Regulation during Enamel Maturation. PloS one. 2015; 10:e0144703. doi:10.1371/journal.pone.0144703. [PubMed: 26671068]

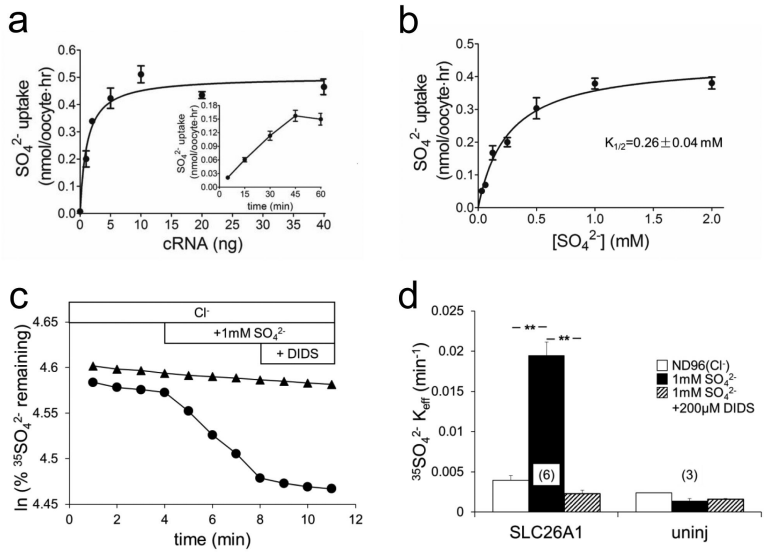

Fig 1. SLC26A1 mediates SO_4^{2-}/SO_4^{2-} exchange

a) SO_4^{2-} uptake by SLC26A1-expressing oocytes saturates at ≥ 5 ng SLC26A1 cRNA (± SE for n=10). (Inset: Time-dependence of SO_4^{2-} uptake by SLC26A1-expressing oocytes (previously injected with 5 ng cRNA) in ND96(Cl^-) containing 1 mM SO_4^{2-} (± SE for n=10)**. b)** Oocytes expressing SLC26A1 (previously injected with 5 ng cRNA) mediate SO_4^{2-} uptake (30 min) from ND96(Cl^-) in a [SO_4^{2-}]-dependent manner. **c)** $^{35}SO_4^{2-}$ efflux traces of representative individual oocytes previously uninjected (triangles) or injected with 5 ng SLC26A1 cRNA (circles) during sequential exposure to ND96(Cl^-), to 1 mM SO_4^{2-} in ND96(Cl^-), and with subsequent addition of 200 µM DIDS. **d)** Mean $^{35}SO_4^{2-}$ efflux rate constants (± SE for n oocytes) from experiments as in panel **c** (**, $p<0.01$)

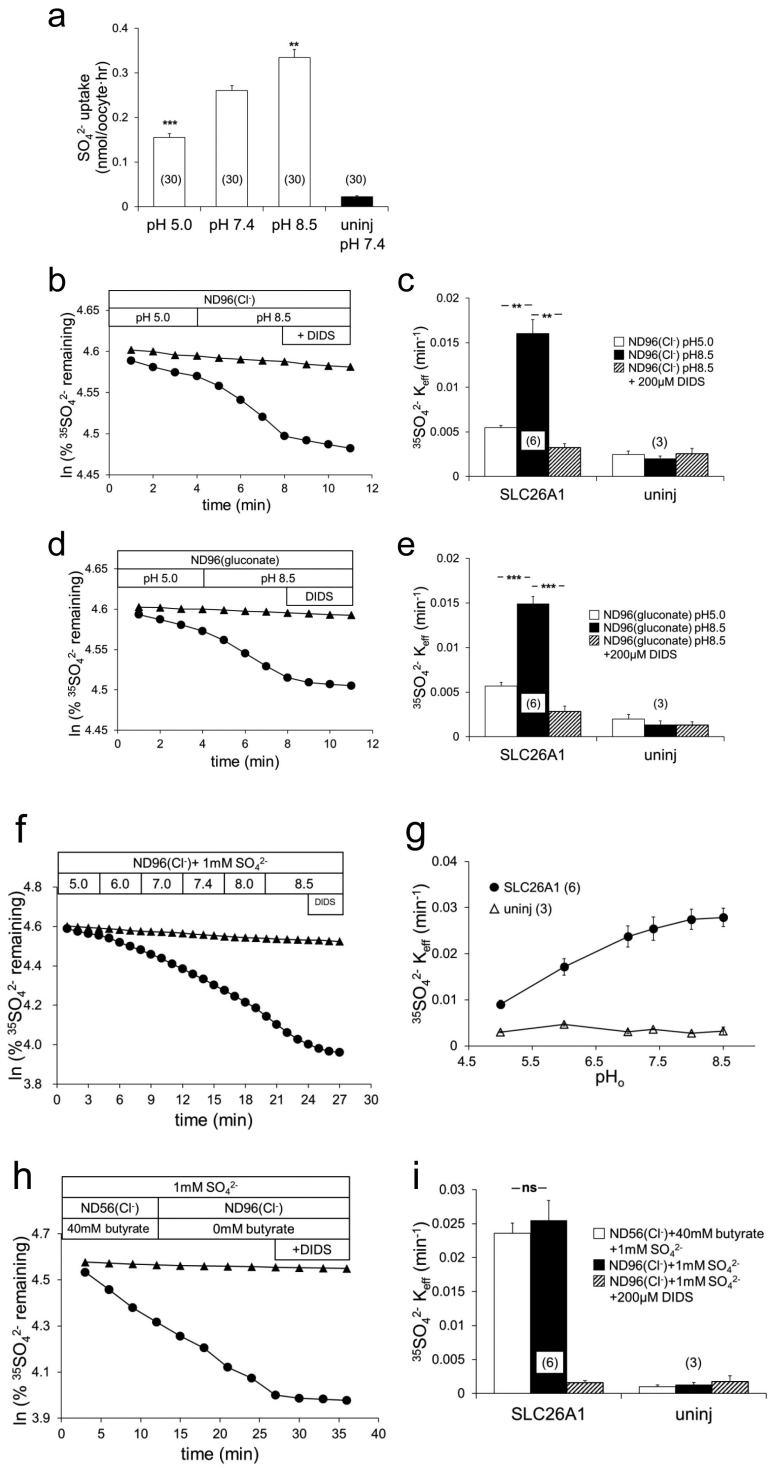

Fig 2. SLC26A1-mediated SO_4^{2-}/anion exchange is regulated by pH_o but not pH_i

a) SLC26A1-mediated SO_4^{2-} uptake from ND96(Cl^-) containing 1 mM SO_4^{2-} at the indicated bath pH values. **b)** $^{35}SO_4^{2-}$ efflux traces of representative individual oocytes previously uninjected (triangles) or injected with 40 ng SLC26A1 cRNA (circles) during sequential exposure to SO_4^{2-}-free ND96(Cl^-) at pH 5.0, pH 8.5 and with subsequent

addition of 200 μM DIDS. **c)** Mean $^{35}SO_4^{2-}$ efflux rate constants from experiments as in panel **b** (± SE for n oocytes). **d)** $^{35}SO_4^{2-}$ efflux traces of representative individual oocytes previously uninjected (triangles) or injected with 40 ng SLC26A1 cRNA (circles) during sequential exposure to Cl^--free, SO_4^{2-}-free ND96(gluconate) at pH 5.0, pH 8.5 and with subsequent addition of 200 μM DIDS. **e)** Mean $^{35}SO_4^{2-}$ efflux rate constants from experiments as in panel **d** (± SE for n oocytes). **f)**$35SO_4^{2-}$ efflux traces of representative individual oocytes previously uninjected (triangles) or injected with 5 ng SLC26A1 cRNA (circles) during sequential exposure to ND96(Cl^-) containing 1 mM SO_4^{2-} baths of the indicated pH values, with subsequent addition of 200 μM DIDS. **g)** Mean pH_o-dependent $^{35}SO_4^{2-}{}_{[i]}/SO_4^{2-}{}_{[o]}$ exchange rate constants from experiments as in panel **f** (± SE for n oocytes). **h)** $^{35}SO_4^{2-}$ efflux traces of representative individual oocytes previously uninjected (triangles) or injected with 5 ng SLC26A1 cRNA (circles), preincubated 30 min with 40 mM Na butyrate in ND56(Cl^-), then exposed sequentially in the presence of 1 mM SO_4^{2-} to ND56(Cl^-) + 40 mM butyrate, to ND96(Cl^-) without butyrate, and with subsequent addition of 200 μM DIDS. **i)** Mean $^{35}SO_4^{2-}$ efflux rate constants (± SE for n oocytes) from experiments as in panel **h** (**, $p<0.01$; ***, $p<0.001$).

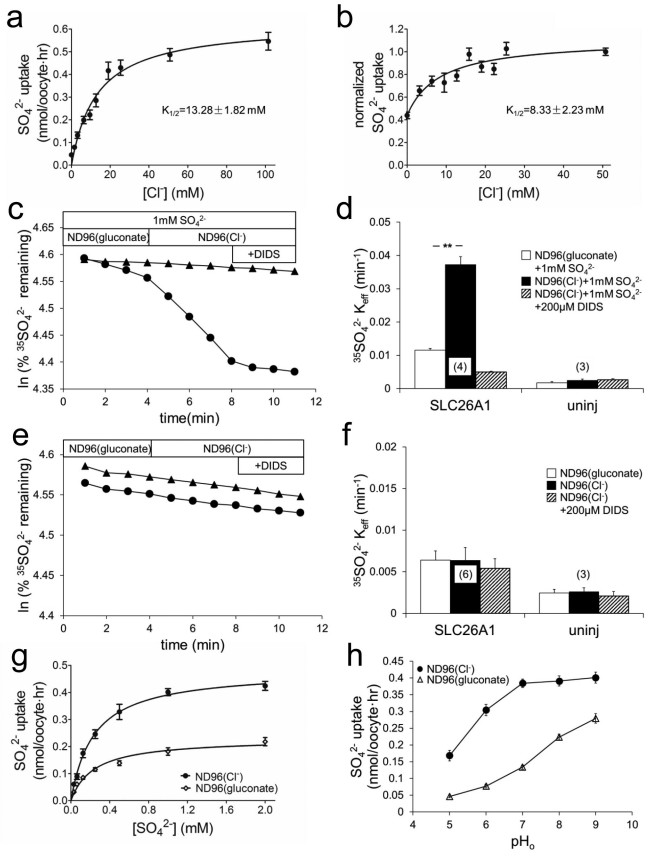

Fig 3. $Cl^-_{[o]}$ cis-stimulates SLC26A1-mediated SO_4^{2-} transport

a) SLC26A1-mediated SO_4^{2-} uptake (5 ng cRNA) from bath solutions containing 1 mM SO_4^{2-} and increasing [Cl^-], with mannitol to balance osmolarity (± SE, n=9-10). **b**) SLC26A1-mediated SO_4^{2-} uptake (5 ng cRNA) from bath solutions containing 1 mM SO_4^{2-} and increasing [Cl^-], with gluconate to balance osmolarity (± SE, n=10-20). **c)** $^{35}SO_4^{2-}$ efflux traces from representative individual oocytes previously uninjected (triangles) or injected with 5 ng SLC26A1 cRNA (circles) during sequential exposure to baths containing 1 mM SO_42 first in ND96(gluconate), then in ND96(Cl^-), with subsequent addition of 200 μM DIDS. **d)** $^{35}SO_4^{2-}$ efflux rate constants from experiments as in panel **c** (mean ± SE for n oocytes). **e)** $^{35}SO_4^{2-}$ efflux traces from representative individual oocytes previously uninjected (triangles) or injected with 40 ng SLC26A1 cRNA (circles) during sequential exposure to SO_4^{2-}-free baths of ND96(gluconate) and ND96(Cl^-), with subsequent addition of 200 μM DIDS. **f)** $^{35}SO_4^{2-}$ efflux rate constants from experiments as in panel **e** (mean ± SE for n oocytes). **g)** SLC26A1-mediated SO_4^{2-} uptake (5 ng cRNA) from ND96(Cl^-) and ND96(gluconate) solutions containing increasing [SO_4^{2-}] as indicated (± SE, n=20). **h)** SLC26A1-mediated SO_4^{2-} uptake (5ng cRNA) in ND96(Cl^-) and ND96(gluconate) solutions containing 1 mM SO_4^{2-} at the indicated pH values (± SE, n=15-16;. **, p<0.01).

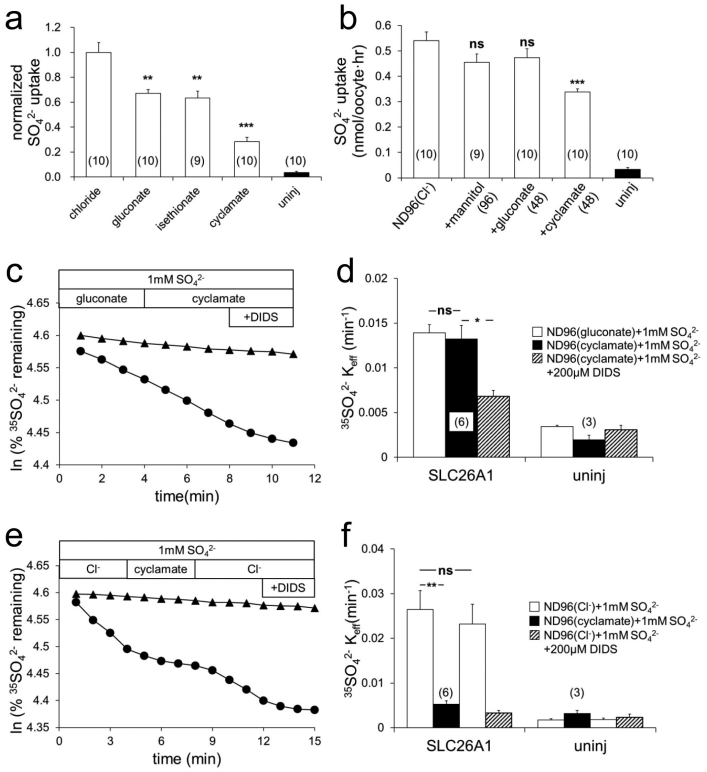

Fig 4. Cyclamate cis-inhibits SLC26A1-mediated SO_4^{2-} influx

a) Normalized SLC26A1-mediated SO_4^{2-} uptake (5 ng cRNA) from bath containing 1 mM SO_4^{2-} in the presence of either ND96(Cl^-) (normalized to 1.0), ND96(gluconate), ND96(isethionate), or ND96(cyclamate). Black bars show uninjected oocytes in ND96(Cl^-) plus 1 mM SO_4^{2-}. **b)** SLC26A1-mediated SO_4^{2-} uptake (5 ng cRNA) from bath containing 1 mM SO_4^{2-} in ND96(Cl^-) or in bath containing 56 mM Cl^- plus either 96 mM D-mannitol, 48 mM gluconate, or 48 mM cyclamate. Black bars show uninjected oocytes in ND96(Cl^-) plus 1 mM SO_4^{2-}. All fluxes in panels a and b were DIDS-sensitive (not shown). **c)** $^{35}SO_4^{2-}$ efflux traces from representative individual uninjected (triangles) and 5 ng SLC26A1 cRNA-injected oocytes (circles) during sequential exposure to bath solutions containing 1 mM SO_4^{2-} in the presence of Cl^--free ND96(gluconate), then ND96(cyclamate), with subsequent addition of 200 μM DIDS. **d)** Mean $^{35}SO_4^{2-}$ efflux rate constants (± SE for n oocytes) as in experiments of panel **c**. **e)** $^{35}SO_4^{2-}$ efflux traces from representative individual uninjected (triangles) and 5 ng SLC26A1 cRNA-injected oocytes (circles) during sequential exposure to bath solutions containing 1 mM SO_4^{2-} in the presence of ND96(Cl^-), ND96(cyclamate), then again ND96(Cl^-), with final addition of 200 μM DIDS. **f)** Mean $^{35}SO_4^{2-}$ efflux rate constants of oocytes (± SE for n oocytes) as in experiments of panel **e** (*, p<0.05; **, p<0.01; ***, p<0.001).

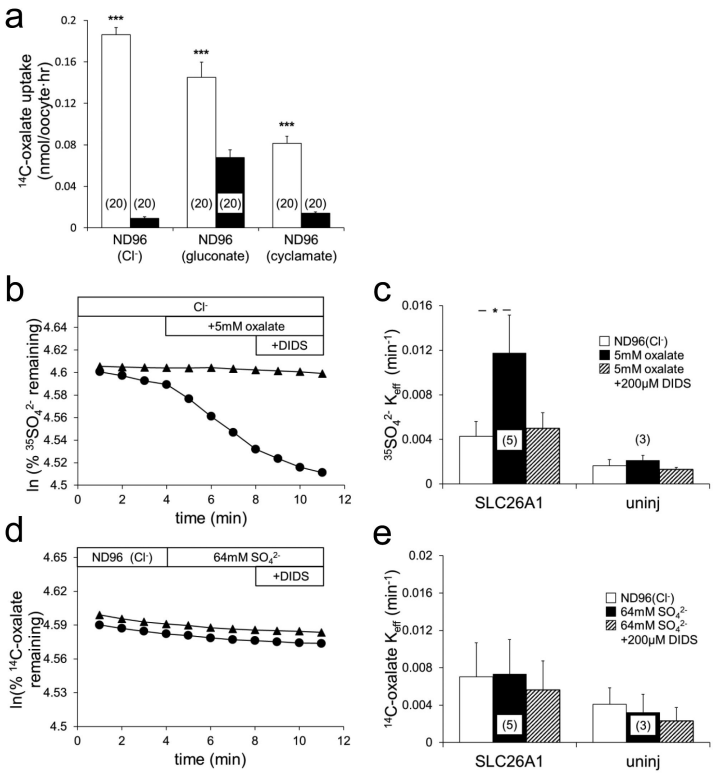

Fig 5. SLC26A1 mediates oxalate transport

a) SLC26A1-mediated ^{14}C-oxalate uptake into oocytes from Ca^{2+}- and Mg^{2+}-free baths containing 1 mM ^{14}C-oxalate in ND96(Cl^-), ND96(gluconate), or ND96(cyclamate) (5 ng cRNA vs. uninjected; n=20, means ± SE). **b)** $^{35}SO_4^{2-}$ efflux traces from representative individual oocytes previously uninjected (triangles) or injected with 5 ng SLC26A1 cRNA (circles), during sequential exposure to Ca^{2+} and Mg^{2+}-free ND96(Cl^-), then to 90.5 mM Cl^- containing 5 mM oxalate, with subsequent addition of 200 μM DIDS. **d)** Mean $^{35}SO_4^{2-}$ efflux rate constants (± SE for n oocytes) from experiments as in panel **c**. **e)** ^{14}C-oxalate efflux traces from representative individual oocytes previously uninjected (triangles) or injected with 40 ng SLC26A1 cRNA (circles) during sequential exposure to ND96(Cl^-), 64mM $^{Na}2^{SO}4$ and subsequent addition of 200 μM DIDS. **f)** Mean 14C-oxalate efflux rate constants (± SE for n oocytes) from experiments as shown in panel **e** (*, p<0.05; ***, p<0.001).

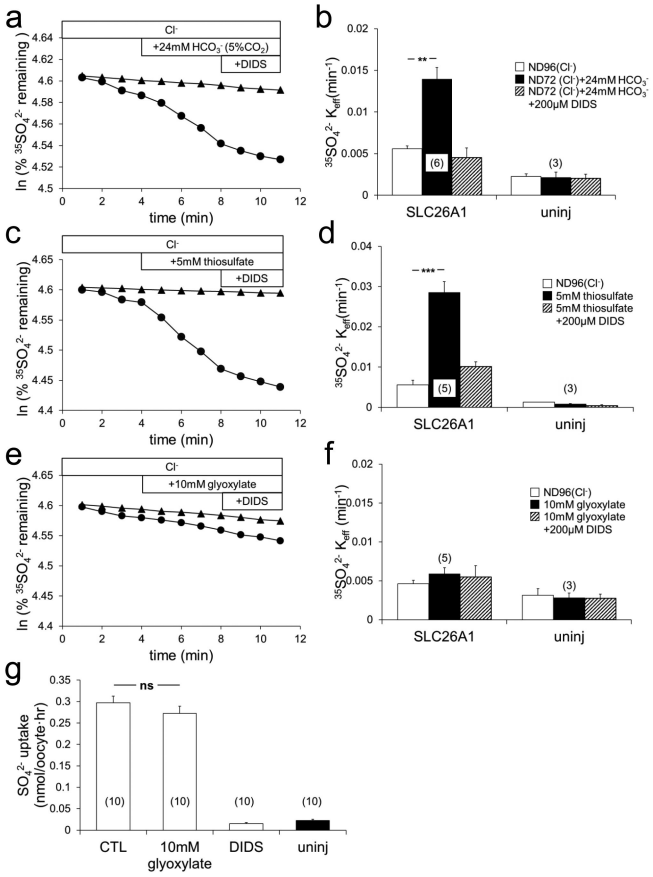

Fig 6. SLC26A1 mediates $^{35}SO_4^{2-}{}_{[i]}/HCO_3^-{}_{[o]}$ exchange and $^{35}SO_4^{2-}{}_{[i]}$/thiosulfate$_{[o]}$ exchange

a) $^{35}SO_4^{2-}$ efflux traces from representative individual oocytes previously uninjected (triangles) or injected with 40 ng SLC26A1 cRNA (circles) during sequential exposure to ND96(Cl^-), then 80 mM Cl^- plus 24 mM HCO_3^-/(5% CO_2), with subsequent addition of 200 μM DIDS. **b)** Mean $^{35}SO_4^{2-}$ efflux rate constants (± SE for n oocytes) from experiments as in panel **a**. **c)** $^{35}SO_4^{2-}$ efflux traces from representative individual oocytes previously uninjected (triangles) or injected with 5 ng SLC26A1 cRNA (circles) during sequential exposure to ND96(Cl^-), then 96 mM Cl^- plus 5 mM sodium thiosulfate, with subsequent addition of 200 μM DIDS. **d)** Mean $^{35}SO_4^{2-}$ efflux rate constants (± SE for n oocytes) from experiments as in panel **c. e)** $^{35}SO_4^{2-}$ efflux traces from representative individual oocytes previously uninjected (triangles) or injected with 40 ng SLC26A1 cRNA (circles) during sequential exposure to ND96(Cl^-), 89 mM Cl^- containing 10 mM glyoxylate, and subsequent addition of 200 μM DIDS. **f)** Mean $^{35}SO_4^{2-}$ efflux rate constants (± SE for n oocytes) from experiments as in panel **e**. **g)** SLC26A1-mediated SO_4^{2-} uptake from baths containing 1 mM SO_4^{2-} in ND96(Cl^-), in 89 mM Cl^- containing 10 mM glyoxylate, and in ND96(Cl^-) containing 200 μM DIDS; Black column shows uninjected oocytes in ND96(Cl^-) (± SE , n=10; **, p<0.01; ***, p<0.001).

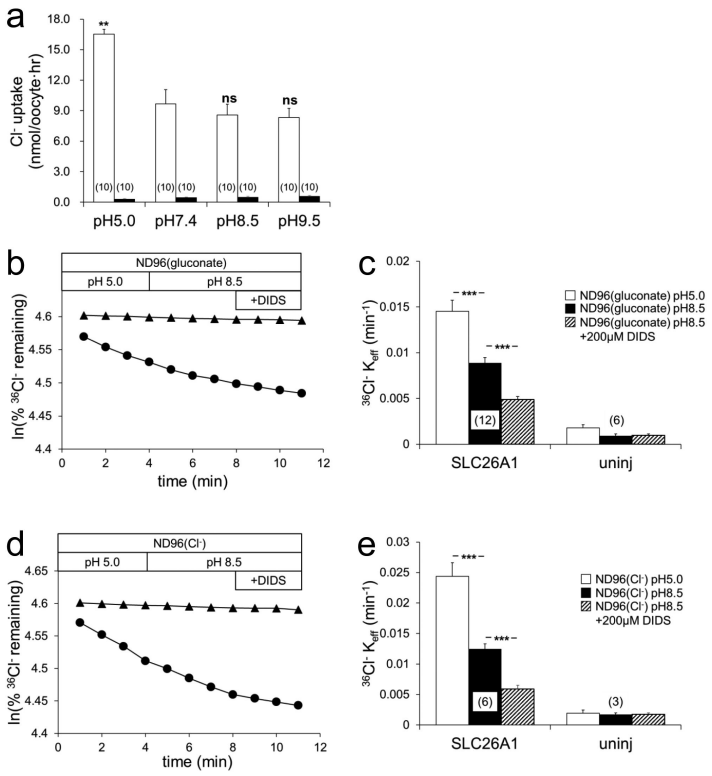

Fig 7. Effects of pH_o on Cl^- flux in SLC26A1-expressing oocytes

a) Cl^- uptake from ND96(Cl^-) at the indicated bath pH_o values into oocytes (± SE, n=10) previously uninjected (black bars) or injected with 40 ng SLC26A1 cRNA (white bars). **b)** $^{36}Cl^-$ efflux traces from representative individual oocytes previously uninjected (triangles) or injected with 40 ng SLC26A1 cRNA (circles) during sequential bath exposure to ND96(gluconate) at pH 5.0, then at pH 8.5, and with subsequent addition of 200 μM DIDS. **c)** Mean $^{36}Cl^-$ efflux rate constants (± SE for n oocytes) from experiments as in panel **b**. **d)** $^{36}Cl^-$ efflux traces from representative individual oocytes previously uninjected (triangles) or injected with 40 ng SLC26A1 cRNA (circles) during sequential bath exposure to ND96(Cl^-) at pH 5.0, then at pH 8.5, and with subsequent addition of 200 μM DIDS. **e)** Mean $^{36}Cl^-$ efflux rate constants (± SE for n oocytes) from experiments as in panel **d** (**, p<0.01; ***, p<0.001).

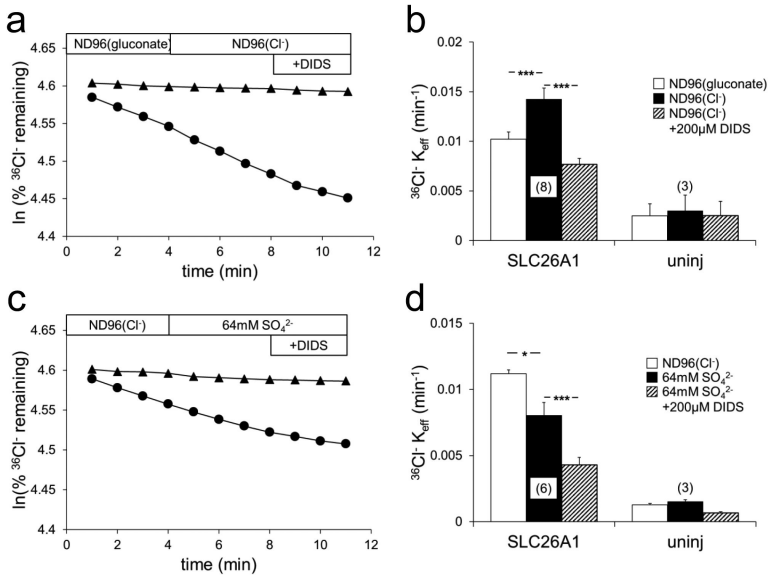

Fig 8. SLC26A1 mediates a small component of $Cl^-_{[i]}/Cl^-_{[o]}$ self-exchange

a) $^{36}Cl^-$ efflux traces from representative individual oocytes previously uninjected (triangles) or injected with 40 ng SLC26A1 cRNA (circles) during sequential exposure to ND96(gluconate) and ND96(Cl^-), with subsequent addition of 200 μM DIDS. **b)** Mean $^{36}Cl^-$ efflux rate constants (± SE for n oocytes) from experiments as in panel **a**. **c)** $^{36}Cl^-$ efflux traces from representative individual oocytes previously uninjected (triangles) or injected with 40 ng SLC26A1 cRNA (circles) during sequential exposure to ND96(Cl^-), then to 64 mM Na_2SO_4, with subsequent addition of 200 μM DIDS. **d)** Mean $^{36}Cl^-$ efflux rate constants (± SE for n oocytes) from experiments as in panel **c** (*, $p<0.05$; ***, $p<0.001$).

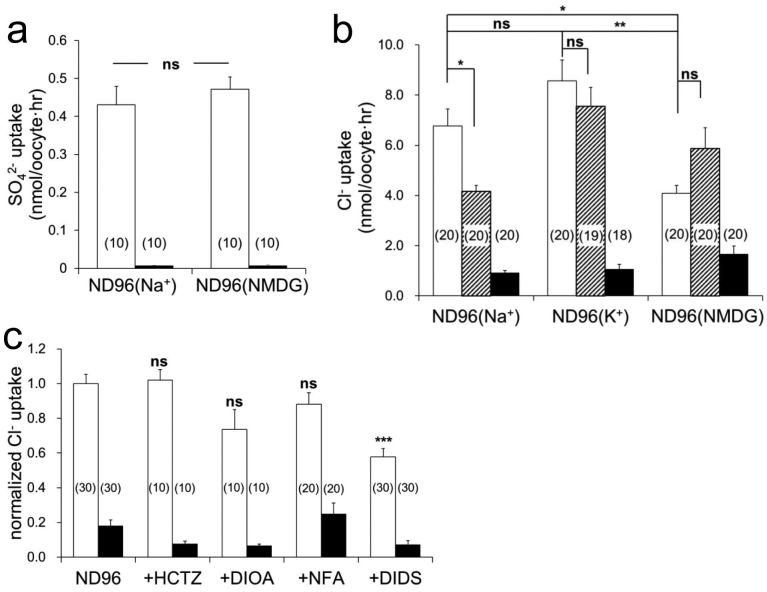

Fig 9. SLC26A1-mediated uptakes of Cl^- and SO_4^{2-} differ in cis-Na+-dependence and apparent DIDS-sensitivity

a) SO_4^{2-} uptake by oocytes (n=10) previously uninjected (black bars) or injected with 5 ng SLC26A1 cRNA (white bars), from baths containing 1 mM SO_4^{2-} in the presence of ND96(Na^+) or ND96(NMDG). **b)** Cl^- uptake by oocytes (n=20) previously uninjected (black bars) or injected with 40 ng SLC26A1 cRNA (white bars), from baths of ND96(Na^+), ND96(K^+), or ND96 (NMDG), in the absence or presence (cross-hatched bars) of 200 μM DIDS. **c)** Normalized SLC26A1-associated Cl^- uptake (40ng cRNA) from ND96 bath in the absence or presence of 500 μM hydrochlorothiazide (HCTZ), 100 μM dihydroindenyloxyalkanoic acid (DIOA), 200 μM niflumic acid (NFA), or 200 μM DIDS (Mean values ± SE for n oocytes are normalized to absence of inhibitor) (*, $p<0.05$; **, $p<0.01$; ***, $p<0.001$).

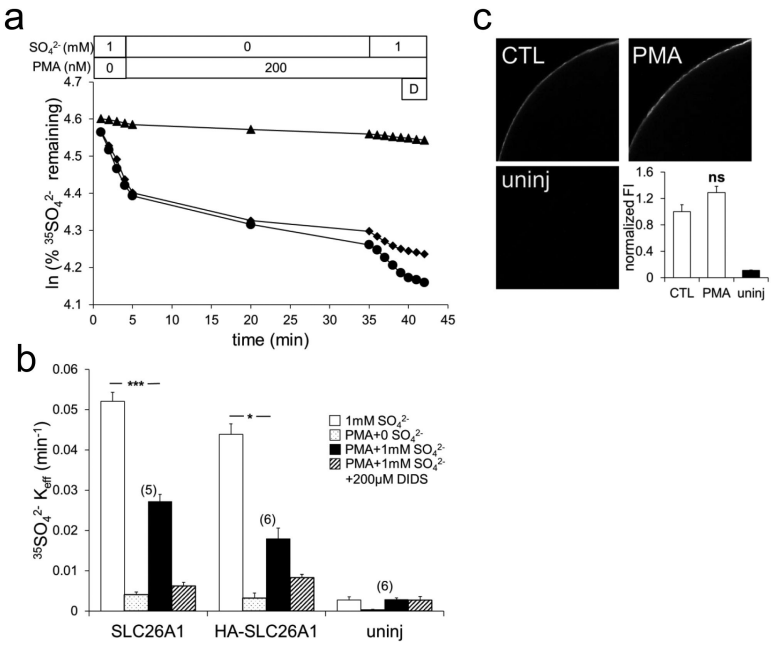

Fig 10. Inhibition of SLC26A1 by phorbol 12-myristate 13-acetate (PMA)

a) $^{35}SO_4^{2-}$ efflux traces from representative individual oocytes uninjected (triangles) or injected with 5 ng SLC26A1 cRNA (circles) or HA-SLC26A1 cRNA (squares) during sequential exposure to ND96(Cl^-) containing 1 mM SO_4^{2-}, then for 30 min to SO_4^{2-}-free ND96(Cl^-) containing 200 nM PMA, followed by readdition of 1 mM SO_4^{2-} to the same bath, and with subsequent addition of 200 µM DIDS. **b)** Mean $^{35}SO_4^{2-}$ efflux rate constants (± SE for n oocytes) from experiments as in panel **a**. **c)** Confocal immunofluorescence micrographs of representative oocytes previously uninjected or injected with 5 ng HA-SLC26A1 cRNA, then incubated in 200nM PMA or DMSO vehicle (CTL) as indicated; lower right: normalized HA-SLC26A1 fluorescence intensity (mean ± SE, n=20) at periphery of oocytes treated with PMA or DMSO (*, $p<0.05$; ***, $p<0.001$).

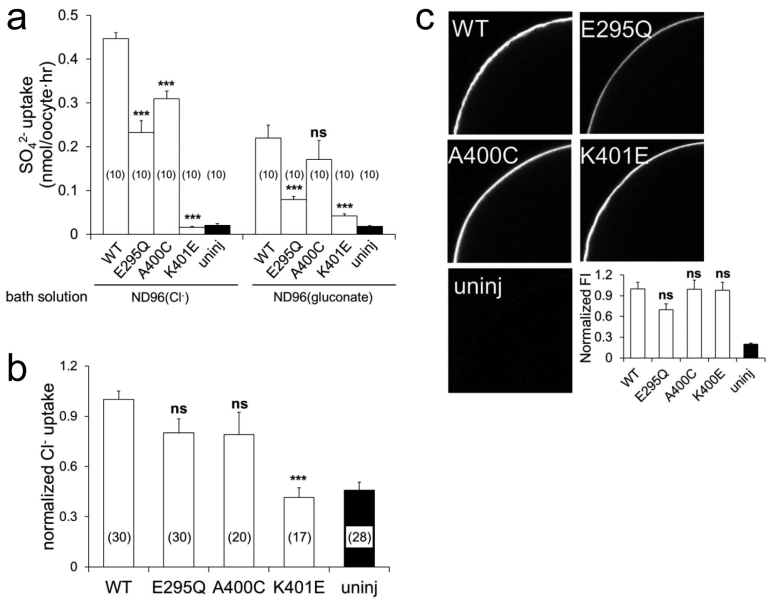

Fig 11. Functional tests of select mutations in highly conserved amino acid residues of SLC26A1

a) SO_4^{2-} uptake from ND96(Cl^-) and from ND96(gluconate) baths containing 1 mM SO_4^{2-} by oocytes (n=10) previously uninjected (black bars) or injected with 5 ng cRNA encoding $SLC26A1^{WT}$ or the indicated mutants (white bars). **b)** Normalized Cl^- influx by oocytes (n=17-30) previously uninjected (black bar) or injected with 5 ng cRNA encoding $SLC26A1^{WT}$ or the indicated mutants (white bars). **c)** Confocal immunofluorescence micrographs of representative oocytes, uninjected or previously injected with 5ng cRNA encoding HA-$SLC26A1^{WT}$ or the indicated HA-tagged mutant cRNAs. Lower right: normalized HA-SLC26A1 fluorescence intensity at the oocyte periphery (mean ± SE, n=20; ***, $p<0.001$).

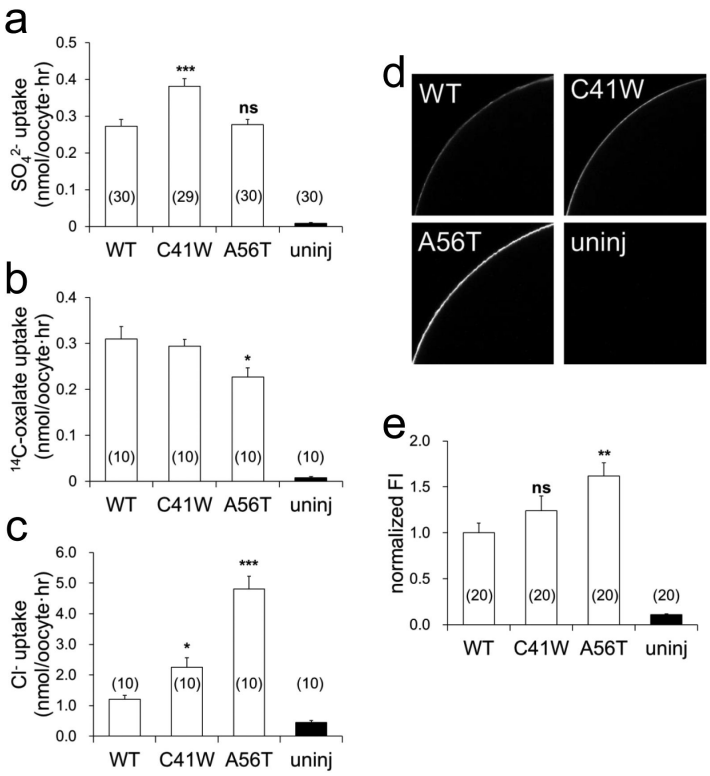

Fig 12. Functional tests of candidate pathological missense variants of SLC26A1

Uptake of SO_4^{2-} (**a**),14C-oxalate (**b**) and Cl^- (**c**) by oocytes (n=10-30) previously uninjected (black bars) or injected with 5 ng cRNA (white bars) encoding SLC26A1^{WT} or compound heterozygous variants SLC26A1^{C41W} or SLC26A1^{A56T} found in a renal Fanconi Syndrome exome. **d)** Confocal immunofluorescence micrographs of representative oocytes previously uninjected or injected with 5ng cRNA encoding HA-SLC26A1^{WT}, HA-SLC26A1^{C41W} or HA-SLC26A1^{A56T}. **e)** Normalized HA-SLC26A1 fluorescence intensity at oocyte periphery (mean ± SE, n=20; *, p<0.05; **, p<0.01; ***, p<0.001).

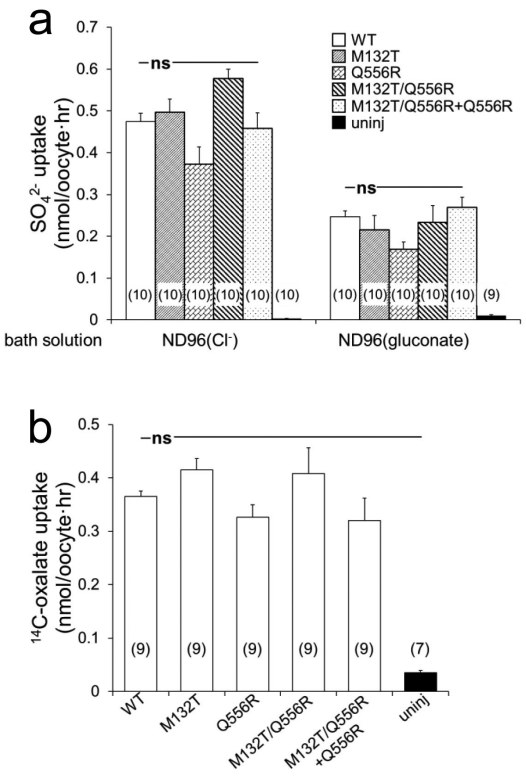

Fig. 13. Functional tests of nephrocalcinosis-associated missense variants of SLC26A1

a) SO_4^{2-} uptake from ND96(Cl^-) or ND96(gluconate) by oocytes previously uninjected (black bar) or injected with 5ng cRNA (white bars) encoding $SLC26A1^{WT}$ or rare variant $SLC26A1^{M132T}$, common variant $SLC26A1^{Q556R}$, nephrolithiasis-associated double variant $SLC26A1^{M132T/Q556R}$, or co-injected with cRNAs (2.5 ng each) encoding $SLC26A1^{M132T/Q556R}$ + $SLC26A1^{Q556R}$ (n=10). An independent experiment comparing only $SLC26A1^{M132T}$ and $SLC26A1^{WT}$ yielded indistinguishable results (n=20, not shown). **b)** ^{14}C-oxalate uptake from ND96(Cl^-) by oocytes previously uninjected (black bar) or injected (white bars) with 5 ng cRNAs (or 2.5 ng each for two cRNAs) encoding the indicated SLC26A1 polypeptide (n=10).

Table 1

Differences between SLC26A1-mediated $SO4^{2-}$ transport and SLC26A1-associated Cl^{-} transport.

	SO_4^{2-} transport	**Cl^- transport**
pHo effects	alkaline pH_o stimulates SO_4^{2-} flux	acidic pHo stimulates Cl- flux
OH-/anion exchange	possible $SO_4^{2-}{}_{[i]}/OH^-{}_{[o]}$ exchange	no detectable $Cl^-{}_{[i]}/OH^-{}_{[o]}$ exchange
Cl^--SO_4^{2-} exchange	no detectable $SO_4^{2-}{}_{[i]}/Cl^-{}_{[o]}$ exchange	possible $Cl\text{-}_{[i]}/SO_4^{2-}{}_{[o]}$ exchange
$Na^+{}_{[o]}$ effects	$Na^+{}_{[o]}$-independent SO_4^{2-} influx	$Na^+{}_{[o]}$-dependent component of Cl^- influx
DIDS-sensitivity	DIDS-sensitive	$Na^+{}_{[o]}$-sensitive component of Cl^- flux is DIDS-sensitive